석사학위논문

Master's Thesis

Warping 변위를 고려한 일반 빔 유한요소의 개발

Development of general beam finite elements for arbitrary section with warping displacements

윤 경 호 (尹 景 虎 Yoon, Kyungho)
기계항공시스템학부 해양시스템공학전공
Division of Ocean Systems Engineering
School of Mechanical, Aerospace and Systems Engineering

KAIST

2011

Warping 변위를 고려한 일반 빔 유한요소의 개발

Development of general beam finite elements for arbitrary section with warping displacements

Development of general beam finite elements for arbitrary section with warping displacements

Advisor : Professor Phill-Seung Lee

Co-advisor : Professor K. C. Park

by

Kyungho Yoon

Division of Ocean Systems Engineering
School of Mechanical, Aerospace and Systems Engineering
KAIST

A thesis submitted to the faculty of KAIST in partial fulfillment of the requirements for the degree of Master of Science in Engineering in the School of Mechanical, Aerospace and Systems Engineering, Division of Ocean Systems Engineering. The study was conducted in accordance with Code of Research Ethics[1]

May 23, 2011

Approved by

Professor Phill-Seung Lee

____

[1]Declaration of Ethical Conduct in Research: I, as a graduate student of KAIST, hereby declare that I have not committed any acts that may damage the credibility of my research. These include, but are not limited to: falsification, thesis written by someone else, distortion of research findings or plagiarism. I affirm that my thesis contains honest conclusions based on my own careful research under the guidance of my thesis advisor.

Development of general beam finite elements for arbitrary section with warping displacements

Kyungho Yoon

The present dissertation has been approved by the dissertation committee as a master's thesis at KAIST

May 23, 2011

Committee head Phill-Seung Lee

Committee member K. C. Park

Committee member Seyoung Im

MOSE
20103413

윤 경 호. Yoon, Kyungho. Development of general finite beam elements for arbitrary section with warping displacements. Warping 변위를 고려한 일반 빔 유한요소의 개발. School if Mechanical, Aerospace and Systems Engineering, Division of Ocean Systems Engineering. 2011. 36p. Advisor Prof. Lee, Phill-Seung, Text in English.

ABSTRACT

In this paper, we suggest method that allows to solve torsional problems of beam structure for arbitrary cross sections. To obtain continuous displacements due to warping effect for arbitrary cross sections, we numerically solve the St.Venant equations and interpolate the solutions through the longitudinal direction of the beam element. Mapping these continuous displacements to standard curved beam displacements, the elements can consider free and restrained warping conditions, eccentric load, varying sections, and curved geometries for arbitrary cross section.

Keywords: FEM, St.Venant, Beam, Torsion, Warping

Table of Contents

Chapter 1. Introduction

Finite beam elements are abundantly used for numerically analyzing behavior of engineering structures. However it yet has any problems to solve torsional problems that standard beam formulations can`t describe twisting deformations. For considering torsion effect, usually beam modeling is replaced by shell or solid elements or ignored. Thus, to develop finite beam elements with warping effect (plane cross-section do not remain plane) is needed. Especially in restrained warping case (prevent the member ends from warping freely), occur distributed axial normal stress at the end. By following this normal stress, St.Venant shear and bi-moment are developed. Thus, we have to solve more complex governing equation than free warping case, and can`t apply to varying section and curved structure case.

Analytical solution of torsional beam problem in free warping case was reported by Timoshenko(1945). Vlasov(1961) established thin-walled beam theory, and obtained solution of restrained warping condition. In succession, Reissner(1979, 1983, 1992) suggested method that can consider coupled load for prismatic beam. Until recent, it was dominantly used for solving torsional problem by FEM that obtain continuous warping function by interpolating warping function at each node with additional warping degree of freedom. In this method, Vlasov(1961) gave analytical warping function(contour warping & thickness warping) for thin-walled beam. And Bathe(1982) suggested for rectangular cross section case. However, these studies applied just simple case that only rectangular or thin-walled cross section.

The purpose of this paper is to develop general beam finite elements with arbitrary cross section for fully-coupled load condition(torsion, bending, stretch) in case of varying section, curved geometry. We suggest inventive formulation of iso-parametric beam elements for arbitrary cross sections. In these formulations, St.Venant solution is needed for obtaining warping displacement fields term. Thus, we introduce method of solving St.Venant equation by using FEM. Lastly, we present various numerical results.

Chapter 2. 3-dimensional curved finite beam elements formulation with arbitrary sections

In this section, introduce displacement based three dimensional curved beam interpolation for arbitrary section (Fig.1), and application of numerical warping function calculated in previous chapter. Lastly, present about integration technique.

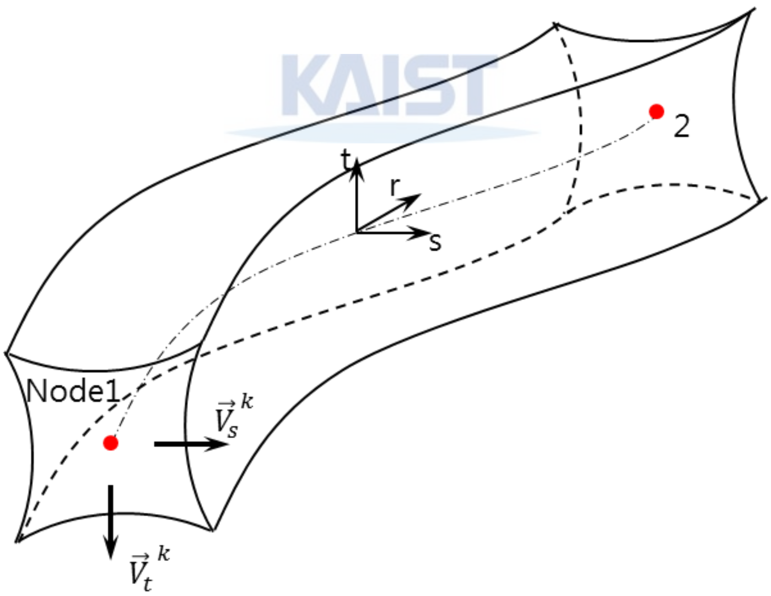

Fig.1. General curved beam element with arbitrary cross-section

2.1 Displacement field for arbitrary sections

First of all, translate coordinate system at twisting center which is obtained in previous chapter. For example of displacement based beam element, interpolation of rectangular section at time l is well known and as following.

x, y, z : Cartesian coordinates of any point in the element

x_i, y_i, z_i : Cartesian coordinates of nodal point i

a_i, b_i : rectangular dimensions

$\overrightarrow{V_s}^i, \overrightarrow{V_t}^i$: unit vector in direction s and t

$h_i(r)$: interpolation function for longitudinal direction

$$\begin{cases} x(r,s,t) = \sum_{i=1}^{k} h_i x_i + \sum_{i=1}^{k} h_i \left(\frac{a_i}{2} t\right) {}^l V_{tx}^i + \sum_{i=1}^{k} h_i \left(\frac{b_i}{2} s\right) {}^l V_{sx}^i \\ y(r,s,t) = \sum_{i=1}^{k} h_i y_i + \sum_{i=1}^{k} h_i \left(\frac{a_i}{2} t\right) {}^l V_{ty}^i + \sum_{i=1}^{k} h_i \left(\frac{b_i}{2} s\right) {}^l V_{sy}^i \\ z(r,s,t) = \sum_{i=1}^{k} h_i z_i + \sum_{i=1}^{k} h_i \left(\frac{a_i}{2} t\right) {}^l V_{tz}^i + \sum_{i=1}^{k} h_i \left(\frac{b_i}{2} s\right) {}^l V_{sz}^i \end{cases} \quad (41)$$

We implement these interpolations for arbitrary section. In rectangular section, y, z directional coordinates are easily mapped by $\frac{b_i}{2}s$, $\frac{a_i}{2}t$, but in arbitrary section are not. For applying at arbitrary section case, we newly introduce sectional node and interpolation (These come from information for calculating warping function in chapter2).

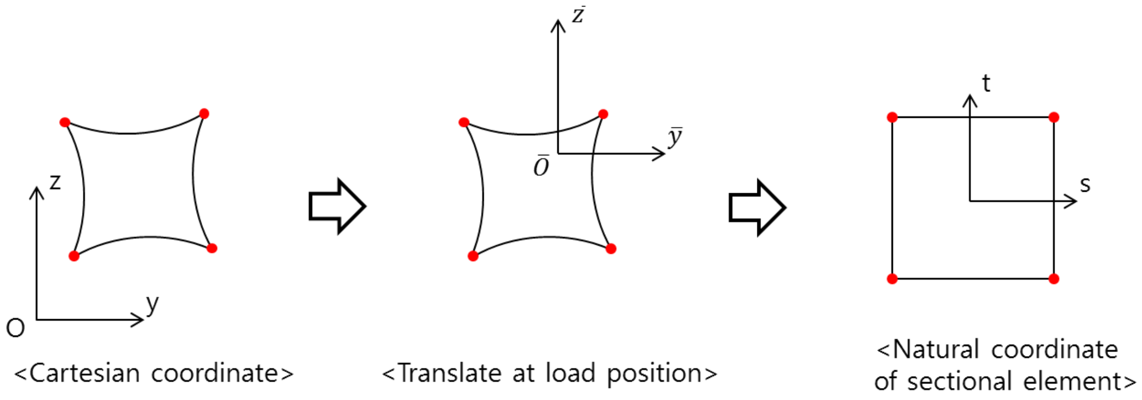

Fig.2. Coordinate change for sectional element

Before interpolate sectional nodes with natural coordinate system, we translate center of initial coordinates to center of load position (coordinate center O mean reference line of beam element). By translating reference line, we can apply eccentric load at that position.

$\bar{Y}, \bar{Z}$: Cartesian coordinates of any point in the element

$\bar{y}_i, \bar{z}_i$: Cartesian coordinates of nodal point i

$\bar{h}_i(s,t)$: interpolation function for sectional element

$$\begin{cases} \bar{Y}(s,t) = \sum_{i=1}^{p} \bar{h}_i(s,t)\,\bar{y}_i \\ \bar{Z}(s,t) = \sum_{i=1}^{p} \bar{h}_i(s,t)\bar{z}_i \end{cases} \tag{42}$$

With above mapping, we can implement interpolation for arbitrary section.

$$\begin{cases} x(r,s,t) = \sum_{i=1}^{k} h_i(r)x_i + \sum_{i=1}^{k} h_i(r)\bar{Z}(s,t)^{l}V_{tx}^{i} + \sum_{i=1}^{k} h_i(r)\bar{Y}(s,t)^{l}V_{sx}^{i} \\ y(r,s,t) = \sum_{i=1}^{k} h_i(r)y_i + \sum_{i=1}^{k} h_i(r)\bar{Z}(s,t)^{l}V_{ty}^{i} + \sum_{i=1}^{k} h_i(r)\bar{Y}(s,t)^{l}V_{sy}^{i} \\ z(r,s,t) = \sum_{i=1}^{k} h_i(r)z_i + \sum_{i=1}^{k} h_i(r)\bar{Z}(s,t)^{l}V_{tz}^{i} + \sum_{i=1}^{k} h_i(r)\bar{Y}(s,t)^{l}V_{sz}^{i} \end{cases} \tag{43}$$

With define terms of displacement and rotation angles.

$$u(r,s,t) = \Delta x\,,\;\; v(r,s,t) = \Delta y\,,\;\; w(r,s,t) = \Delta z$$

$$\theta_k = \begin{bmatrix}\theta_x^k & \theta_y^k & \theta_z^k\end{bmatrix}^T$$

$$\begin{cases} V_t^k = {}^{1}V_t^k - {}^{0}V_t^k = \theta_k \times {}^{0}V_t^k \\ V_s^k = {}^{1}V_s^k - {}^{0}V_s^k = \theta_k \times {}^{0}V_s^k \end{cases} \tag{44}$$

Finally we obtain the standard displacement field of general curved beam element for arbitrary section with 6 degree of freedom displacement vector $\vec{u} = [u \quad v \quad w \quad \theta_x \quad \theta_y \quad \theta_z]^T$.

$$\begin{cases} u(r,s,t) = \sum_{i=1}^{k} h_i(r)u_i + \sum_{i=1}^{k} h_i(r)\bar{Z}(s,t)(\theta_k \times V_{tx}^{i}) + \sum_{i=1}^{k} h_i(r)\bar{Y}(s,t)(\theta_k \times V_{sx}^{i}) \\ v(r,s,t) = \sum_{i=1}^{k} h_i(r)v_i + \sum_{i=1}^{k} h_i(r)\bar{Z}(s,t)(\theta_k \times V_{ty}^{i}) + \sum_{i=1}^{k} h_i(r)\bar{Y}(s,t)(\theta_k \times V_{sy}^{i}) \\ w(r,s,t) = \sum_{i=1}^{k} h_i(r)w_i + \sum_{i=1}^{k} h_i(r)\bar{Z}(s,t)(\theta_k \times V_{tz}^{i}) + \sum_{i=1}^{k} h_i(r)\bar{Y}(s,t)(\theta_k \times V_{sz}^{i}) \end{cases} \tag{45}$$

This beam formulation has limitation that cannot describe sectional warping displacement. Because beam finite elements have common assumption which is cross-section has to remain in plane. Thus, we superpose additional displacement field for sectional warping. These displacement fields are obtained by interpolation of warping function which is calculated in chapter 2. Detail explanation is presented in next section.

2.2 Application of numerical warping function

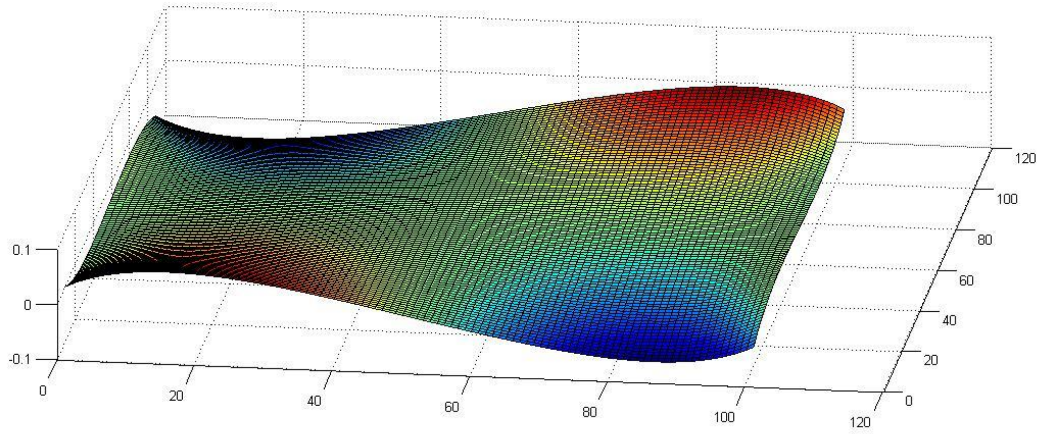

Fig.3. Warping displacement field of rectangular section

As mentioned in chapter2, with assumption $k = \frac{d\theta_x}{dx}$ is constant (prismatic beam), sectional warping displacement field is as following. (Fig.3 is example of warping displacement field)

u_w : Cartesian coordinate of warping displacement

ψ : Cartesian coordinate of warping function

$\overrightarrow{V_r^i}$: *unit vector in direction r*

$$u_w(s,t) = k \cdot \tilde{\psi}(s,t) \cdot V_r^i \qquad (46)$$

Above displacement field is only validated with prismatic beam condition. Thus we define additional warping degree of freedom α each elemental nodes.

$$u_w(s,t) = \sum_{i=1}^{k} \tilde{\psi}(s,t) \cdot V_r^i \cdot h_i(r) \cdot \alpha_i \qquad (47)$$

By this interpolation, we obtain continuous warping function which can implement various beam condition. (non-uniform torsion, curved geometry, varying section)

We apply this continuous warping displacement field to standard displacement filed mentioned in previous section. Then, we obtain final form with 7 degree of freedom at each elemental nodes as following. $\vec{u} = [u \quad v \quad w \quad \theta_x \quad \theta_y \quad \theta_z \quad \alpha]^T$

$$\begin{cases} \mathrm{u}(\mathrm{r},\mathrm{s},\mathrm{t}) = \sum_{\mathrm{i}=1}^{\mathrm{k}} \mathrm{h_i}(r)\mathrm{u_i} + \sum_{\mathrm{i}=1}^{\mathrm{k}} \mathrm{h_i}(r)\bar{Z}(\mathrm{s},\mathrm{t})(\theta_\mathrm{k} \times \mathrm{V_{tx}^i}) + \sum_{\mathrm{i}=1}^{\mathrm{k}} \mathrm{h_i}(r)\bar{Y}(\mathrm{s},\mathrm{t})(\theta_\mathrm{k} \times \mathrm{V_{sx}^i}) + \sum_{i=1}^{k} \psi(\mathrm{s},\mathrm{t}) \cdot \mathrm{V}_{\mathrm{rx}}^{i} \cdot \mathrm{h_i}(r) \cdot \alpha_i \\ \mathrm{v}(\mathrm{r},\mathrm{s},\mathrm{t}) = \sum_{\mathrm{i}=1}^{\mathrm{k}} \mathrm{h_i}(r)\mathrm{v_i} + \sum_{\mathrm{i}=1}^{\mathrm{k}} \mathrm{h_i}(r)\bar{Z}(\mathrm{s},\mathrm{t})(\theta_\mathrm{k} \times \mathrm{V_{ty}^i}) + \sum_{\mathrm{i}=1}^{\mathrm{k}} \mathrm{h_i}(r)\bar{Y}(\mathrm{s},\mathrm{t})(\theta_\mathrm{k} \times \mathrm{V_{sy}^i}) + \sum_{i=1}^{k} \psi(\mathrm{s},\mathrm{t}) \cdot \mathrm{V}_{\mathrm{ry}}^{i} \cdot \mathrm{h_i}(r) \cdot \alpha_i \\ \mathrm{w}(\mathrm{r},\mathrm{s},\mathrm{t}) = \sum_{\mathrm{i}=1}^{\mathrm{k}} \mathrm{h_i}(r)\mathrm{w_i} + \sum_{\mathrm{i}=1}^{\mathrm{k}} \mathrm{h_i}(r)\bar{Z}(\mathrm{s},\mathrm{t})(\theta_\mathrm{k} \times \mathrm{V_{tz}^i}) + \sum_{\mathrm{i}=1}^{\mathrm{k}} \mathrm{h_i}(r)\bar{Y}(\mathrm{s},\mathrm{t})(\theta_\mathrm{k} \times \mathrm{V_{sz}^i}) + \sum_{i=1}^{k} \psi(\mathrm{s},\mathrm{t}) \cdot \mathrm{V}_{\mathrm{rz}}^{i} \cdot \mathrm{h_i}(r) \cdot \alpha_i \end{cases} \tag{48}$$

This displacement field can describe fully-coupled deformation (stretch, bending, torsion) for arbitrary section.

2.3 Finite elements modeling

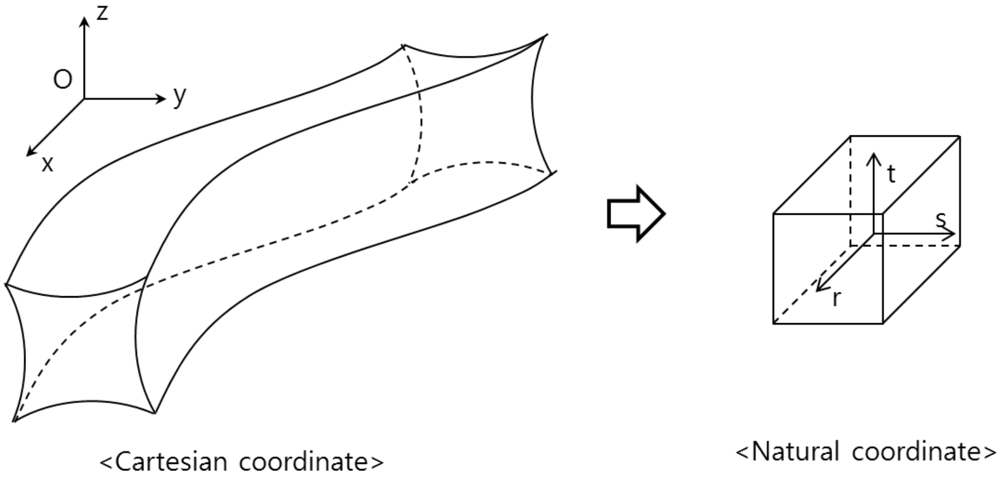

Fig.4. Mapping of coordinate system

For finite elements modeling, firstly we introduce jacobian operator J.

x_i, y_i, z_i : Cartesian coordinates of nodal point i

$\overrightarrow{V_s}^i, \overrightarrow{V_t}^i$: unit vector in direction s and t

$h_i(r)$: interpolation function for longitudinal direction

$\bar{Y}, \bar{Z}$: Cartesian coordinates of any point in section element

$\bar{y_\iota}, \bar{z_\iota}$: Cartesian coordinates of nodal point i

$\overline{h_\iota}(s,t)$: interpolation function for sectional element

$$J = \begin{bmatrix} \frac{\partial x}{\partial r} & \frac{\partial y}{\partial r} & \frac{\partial z}{\partial r} \\ \frac{\partial x}{\partial s} & \frac{\partial y}{\partial s} & \frac{\partial z}{\partial s} \\ \frac{\partial x}{\partial t} & \frac{\partial y}{\partial t} & \frac{\partial z}{\partial t} \end{bmatrix} = \sum_{i=1}^{k} \begin{bmatrix} \frac{\partial h_i}{\partial r} & \frac{\partial h_i}{\partial r}\bar{Z_\iota} & \frac{\partial h_i}{\partial r}\bar{Y_\iota} \\ 0 & h_i\frac{\partial \bar{Z_\iota}}{\partial s} & h_i\frac{\partial \bar{Y_\iota}}{\partial s} \\ 0 & h_i\frac{\partial \bar{Z_\iota}}{\partial t} & h_i\frac{\partial \bar{Y_\iota}}{\partial t} \end{bmatrix} \begin{bmatrix} x_i & y_i & z_i \\ V_{tx}^i & V_{ty}^i & V_{tz}^i \\ V_{sx}^i & V_{sy}^i & V_{sz}^i \end{bmatrix} \tag{49}$$

With above jacobian matrix and differentiation of displacements respect to natural coordinate, we can change displacement field respect to Cartesian coordinate.

$$\begin{bmatrix} \frac{\partial u}{\partial x} \\ \frac{\partial u}{\partial y} \\ \frac{\partial u}{\partial z} \end{bmatrix} = J^{-1} \begin{bmatrix} \frac{\partial u}{\partial r} \\ \frac{\partial u}{\partial s} \\ \frac{\partial u}{\partial t} \end{bmatrix}, \qquad \begin{bmatrix} \frac{\partial v}{\partial x} \\ \frac{\partial v}{\partial y} \\ \frac{\partial v}{\partial z} \end{bmatrix} = J^{-1} \begin{bmatrix} \frac{\partial v}{\partial r} \\ \frac{\partial v}{\partial s} \\ \frac{\partial v}{\partial t} \end{bmatrix}, \qquad \begin{bmatrix} \frac{\partial w}{\partial x} \\ \frac{\partial w}{\partial y} \\ \frac{\partial w}{\partial z} \end{bmatrix} = J^{-1} \begin{bmatrix} \frac{\partial w}{\partial r} \\ \frac{\partial w}{\partial s} \\ \frac{\partial w}{\partial t} \end{bmatrix} \tag{50}$$

Finally, obtain strain matrix.

$$\begin{bmatrix} \varepsilon_{xx} \\ \varepsilon_{yy} \\ \varepsilon_{zz} \\ \gamma_{xy} \\ \gamma_{yz} \\ \gamma_{zx} \end{bmatrix} = \begin{bmatrix} \frac{\partial u}{\partial x} \\ \frac{\partial v}{\partial y} \\ \frac{\partial w}{\partial z} \\ \frac{\partial u}{\partial y} + \frac{\partial v}{\partial x} \\ \frac{\partial v}{\partial z} + \frac{\partial w}{\partial y} \\ \frac{\partial w}{\partial x} + \frac{\partial u}{\partial z} \end{bmatrix} \tag{51}$$

2.4 Numerical integration

For obtaining stiffness matrix, we integrate strain matrix with material law matrix. Displacement based formulation, which we use, encounter 'shear locking' problem. For releasing 'shear locking', we apply reduced integral technique which is mathematically equal with MITC technique in beam interpolation. Because 3-dimensional curved beam finite elements have only 1-dimensional interpolation function. (longitudinal direction 'r')

For integrating eccentric stiffness matrix, just input s and t gauss point in natural coordinate, we obtain eccentric $\bar{Y}, \bar{Z}$. Example of L-section (multi-elements case) is in Fig.5.

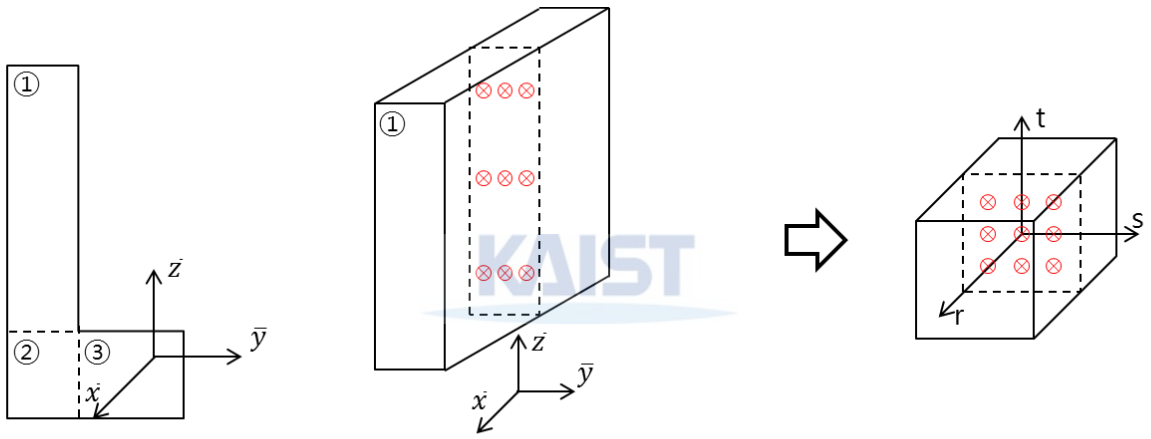

Fig.5. Example of gauss quadrature points for multi-elements case

Chapter 3. Numerical solution of warping function

There are many numerical schemes to obtain St.Venant solutions. However we solve the equation own method by FEM. In this section, we introduce St.Venant equation which is governing equation of twisting section, derive variational formulation of St.Venant equation, and obtain warping displacement field by solving the formulation with finite element method. Finally, find coordinate of twisting center with pre-calculated solution of St.Venant. Obtained displacement field map onto displacement field of standard beam formulation. Detail procedure is as in the following.

3.1 St.Venant Equation and variational formulation

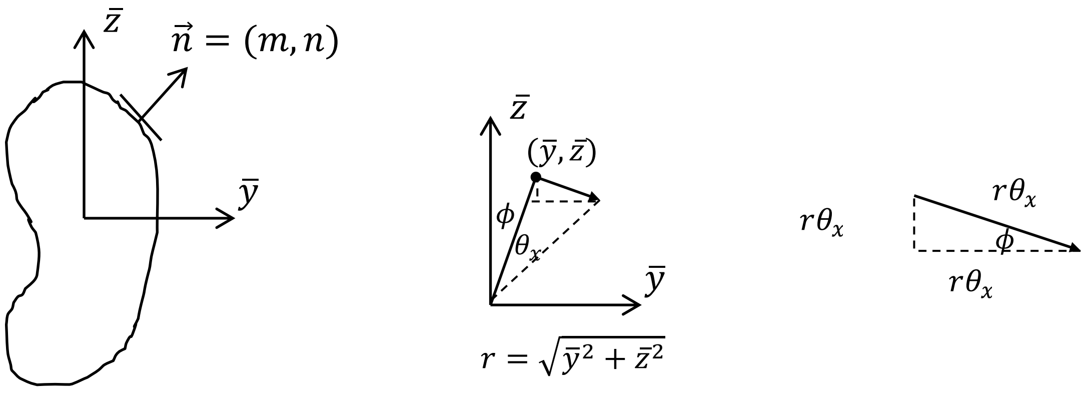

Fig.6. Kinematics of twisting displacement

By fig.6 and defining warping function, we can obtain displacement field. Warping function ψ is defined as longitudinal displacement of cross section. Assume that beam is subjected by constant moments.

$$k = \frac{d\theta_x}{dx} = \text{const.} \quad \theta_x = kx \tag{1}$$

$$u = k \times \psi(\bar{y}, \bar{z})$$

$$v = \bar{z}\theta_x \tag{2}$$

$$w = -\bar{y}\theta_x$$

Above defined displacements, we can calculate strain and stress.

$$\begin{bmatrix} \sigma_{xx} \\ \sigma_{yy} \\ \sigma_{zz} \\ \sigma_{xy} \\ \sigma_{yz} \\ \sigma_{zx} \end{bmatrix} = \begin{bmatrix} E\varepsilon_{xx} \\ E\varepsilon_{yy} \\ E\varepsilon_{zz} \\ G\varepsilon_{xy} \\ G\varepsilon_{yz} \\ G\varepsilon_{zx} \end{bmatrix} = \begin{bmatrix} 0 \\ 0 \\ 0 \\ Gk(\bar{z} + \frac{\partial\psi}{\partial\bar{y}}) \\ 0 \\ Gk(-\bar{y} + \frac{\partial\psi}{\partial\bar{z}}) \end{bmatrix} \tag{3}$$

Apply above stress into local equilibrium state.

$$\begin{cases} \frac{\partial\sigma_{xx}}{\partial x} + \frac{\partial\sigma_{x\bar{y}}}{\partial\bar{y}} + \frac{\partial\sigma_{x\bar{z}}}{\partial\bar{z}} = 0 & \Longrightarrow \quad Gk\left(\frac{\partial^2\psi}{\partial\bar{y}^2} + \frac{\partial^2\psi}{\partial\bar{z}^2}\right) = 0 \\ \frac{\partial\sigma_{\bar{y}x}}{\partial x} + \frac{\partial\sigma_{\bar{y}\bar{y}}}{\partial\bar{y}} + \frac{\partial\sigma_{\bar{y}\bar{z}}}{\partial\bar{z}} = 0 & \Longrightarrow \quad \text{Identity Equation} \\ \frac{\partial\sigma_{\bar{z}x}}{\partial x} + \frac{\partial\sigma_{\bar{z}\bar{y}}}{\partial\bar{y}} + \frac{\partial\sigma_{\bar{z}\bar{z}}}{\partial\bar{z}} = 0 & \Longrightarrow \quad \text{Identity Equation} \end{cases} \tag{4}$$

By kinematics and local equilibrium equation, we obtain Laplace equation. Also boundary condition, which means zero outward stress of surface, is as following. ($\vec{n} = (m, n)$ is outward unit vector of surface in Fig.1)

$$\sigma \cdot \vec{n} = 0 \quad \text{on} \quad \partial\Omega \tag{5}$$

$$m\sigma_{x\bar{y}} + n\sigma_{x\bar{z}} = 0 \tag{6}$$

$$mGk\left(\bar{z} + \frac{\partial\psi}{\partial\bar{y}}\right) + nGk\left(-\bar{y} + \frac{\partial\psi}{\partial\bar{z}}\right) = 0 \tag{7}$$

$$m\frac{\partial\psi}{\partial\bar{y}} + n\frac{\partial\psi}{\partial\bar{z}} = m\bar{z} - n\bar{y} \tag{8}$$

As above, Laplace equation and boundary condition give us St.Venant equation which is governing equation of twisting deformation.

$$\frac{\partial^2\psi}{\partial\bar{y}^2}+\frac{\partial^2\psi}{\partial\bar{z}^2}=0 \quad \text{with B.C.} \qquad \vec{n}\cdot\nabla\psi = m\bar{z}-n\bar{y} \tag{9}$$

This governing equation has limitation of valid only with constant moment with assuming $k=\frac{\partial\theta_x}{\partial x}$ is constant. Thus, distributed torsion problem and restrained warping problem has different governing equation. For solving these problems, we apply technique which is to interpolate k with each elemental node. Explain in detail is presented in beam formulation chapter.

Introduce variation of warping function $\delta\psi$, and derive variational formulation as following.

$$\int\left(\frac{\partial^2\psi}{\partial\bar{y}^2}+\frac{\partial^2\psi}{\partial\bar{z}^2}\right)\delta\psi \;\; dV=0 \tag{10}$$

$$\int\left(\frac{\partial}{\partial\bar{y}}\left(\frac{\partial\psi}{\partial\bar{y}}\delta\psi\right)-\frac{\partial\psi}{\partial\bar{y}}\frac{\partial\delta\psi}{\partial\bar{y}}\right)+\left(\frac{\partial}{\partial\bar{z}}\left(\frac{\partial\psi}{\partial\bar{z}}\delta\psi\right)-\frac{\partial\psi}{\partial\bar{z}}\frac{\partial\delta\psi}{\partial\bar{z}}\right) \; dV=0 \tag{11}$$

$$\int\left(\frac{\partial}{\partial\bar{y}}\left(\frac{\partial\psi}{\partial\bar{y}}\delta\psi\right)+\frac{\partial}{\partial\bar{z}}\left(\frac{\partial\psi}{\partial\bar{z}}\delta\psi\right)\right) \; dV-\int\left(\frac{\partial\psi}{\partial\bar{y}}\frac{\partial\delta\psi}{\partial\bar{y}}+\frac{\partial\psi}{\partial\bar{z}}\frac{\partial\delta\psi}{\partial\bar{z}}\right) \; dV=0 \tag{12}$$

$$\int\left(\frac{\partial\psi}{\partial\bar{y}}\frac{\partial\delta\psi}{\partial\bar{y}}+\frac{\partial\psi}{\partial\bar{z}}\frac{\partial\delta\psi}{\partial\bar{z}}\right) \; dV=\int\left(m\frac{\partial\psi}{\partial\bar{y}}\delta\psi+n\frac{\partial\psi}{\partial\bar{z}}\delta\psi\right) \; dS \tag{13}$$

$$\int\left(\frac{\partial\psi}{\partial\bar{y}}\frac{\partial\delta\psi}{\partial\bar{y}}+\frac{\partial\psi}{\partial\bar{z}}\frac{\partial\delta\psi}{\partial\bar{z}}\right) \; dV=\int(m\bar{z}-n\bar{y})\delta\psi \;\; dS \tag{14}$$

3.2 Finite element model of cross-section

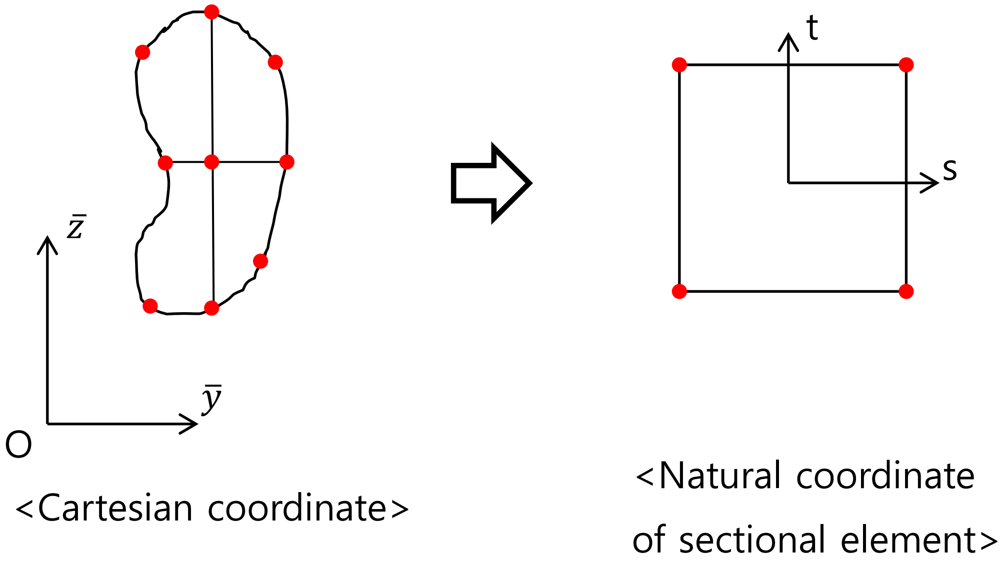

Fig.7. Sectional finite element model for solving St.Venant equation

Using the natural coordinate system of sectional element, we interpolate warping function respect to Cartesian coordinates with k nodal point.

$$\psi(s,t) = \sum_{i=1}^{k} \bar{h}_i(s,t)\psi_i \tag{15}$$

Where the $h_k(s,t)$ are the shape functions, and ψ_k are nodal value of warping function. Also we introduce jacobian operator J which map Cartesian coordinate onto natural coordinate.

$$J = \begin{bmatrix} \frac{\partial \bar{y}}{\partial s} & \frac{\partial \bar{z}}{\partial s} \\ \frac{\partial \bar{y}}{\partial t} & \frac{\partial \bar{z}}{\partial t} \end{bmatrix} = \sum_{i=1}^{k} \begin{bmatrix} \frac{\partial \bar{h}_i}{\partial s} \\ \frac{\partial \bar{h}_i}{\partial t} \end{bmatrix} [\bar{y}_i \quad \bar{z}_i] \tag{16}$$

With above jacobian operator and differentiation of ψ respect to natural coordinate, we can obtain derivation of ψ in Cartesian coordinate as following.

$$\begin{bmatrix} \frac{\partial\psi}{\partial\bar{y}} \\ \frac{\partial\psi}{\partial\bar{z}} \end{bmatrix} = J^{-1} \begin{bmatrix} \frac{\partial\psi}{\partial s} \\ \frac{\partial\psi}{\partial t} \end{bmatrix} = \sum_{i=1}^{k} J^{-1} \begin{bmatrix} \frac{\partial\bar{h}_1}{\partial s} \\ \frac{\partial\bar{h}_1}{\partial t} \end{bmatrix} [\psi_i] \tag{17}$$

By above differential matrix of warping function, obtain matrix form of L.H.S of variational formulation (e.q.[14])

$$\int (\frac{\partial\psi}{\partial\bar{y}}\frac{\partial\delta\psi}{\partial\bar{y}} + \frac{\partial\psi}{\partial\bar{z}}\frac{\partial\delta\psi}{\partial\bar{z}})\ dV = \int \left(\frac{\partial\psi}{\partial\bar{y}}\frac{\partial\delta\psi}{\partial\bar{y}} + \frac{\partial\psi}{\partial\bar{z}}\frac{\partial\delta\psi}{\partial\bar{z}}\right) |\det J| ds dt \tag{18}$$

Lastly, we derive matrix form of R.H.S of variational formulation (e.q.[14]), (boundary condition term). We operate at each boundary face in natural coordinate system.

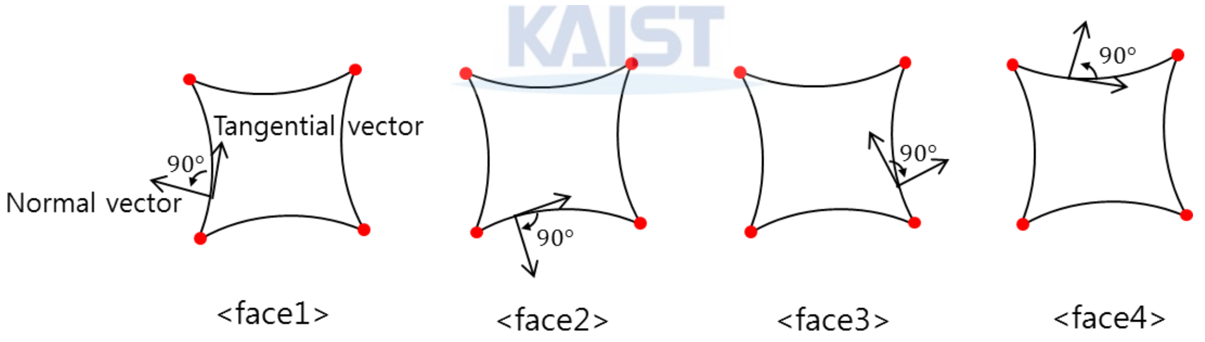

Fig.8. outward normal vector for elemental surface

We can obtain outward normal vector for general curved surface (Fig.8) and changing domain of surface line integration as following.

① Outward normal vector & coordinate change at face1 ($\text{at}\ s = -1\ \&\ t = [-1,1]$)

$$\frac{d\bar{y}}{d\bar{z}} = \frac{\partial\bar{y}}{\partial s}\frac{ds}{d\bar{z}} + \frac{\partial\bar{y}}{\partial t}\frac{dt}{d\bar{z}} = \frac{\frac{\partial\bar{y}}{\partial t}}{\frac{\partial\bar{z}}{\partial t}} = \frac{\sum\frac{\partial\bar{h}_1}{\partial t}\bar{y}_i}{\sum\frac{\partial\bar{h}_1}{\partial t}\bar{z}_i} \qquad (\because\ \frac{d\bar{z}}{dt} = \frac{\partial\bar{z}}{\partial s}\frac{ds}{dt} + \frac{\partial\bar{z}}{\partial t}\frac{dt}{dt} = \frac{\partial\bar{z}}{\partial t}) \tag{19}$$

By above differentiation, we can get slope (tangential vector) of surface curve.

tangential vector ： $\left(\frac{d\bar{y}}{d\bar{z}}, 1\right)$

By rotating tangential vector C.C.W (Fig.3), we can obtain outward normal vector.

normal vector ： $(-1, \frac{d\bar{y}}{d\bar{z}})$

Change differential domain Cartesian coordinate to natural coordinate.

$$dS = \sqrt{(d\bar{y})^2 + (d\bar{z})^2} = \sqrt{\left(\frac{d\bar{y}}{d\bar{z}}\right)^2 + 1}\ d\bar{z} = \sqrt{\left(\frac{d\bar{y}}{d\bar{z}}\right)^2 + 1}\ \frac{d\bar{z}}{dt}\ dt = \sqrt{\left(\frac{\sum\frac{\partial\bar{h}_i}{\partial t}\bar{y}_i}{\sum\frac{\partial\bar{h}_i}{\partial t}\bar{z}_i}\right)^2 + 1}\ \left(\sum\frac{\partial\bar{h}_i}{\partial t}\bar{z}_i\right) dt \tag{20}$$

② Outward normal vector & coordinate change at face2 ($\text{at } t = -1 \ \& \ s = [-1,1]$)

$$\frac{d\bar{z}}{d\bar{y}} = \frac{\partial \bar{z}}{\partial s}\frac{ds}{d\bar{y}} + \frac{\partial \bar{z}}{\partial t}\frac{dt}{d\bar{y}} = \frac{\frac{\partial \bar{z}}{\partial s}}{\frac{\partial \bar{y}}{\partial s}} = \frac{\sum \frac{\partial \overline{h_1}}{\partial s}\bar{z}_i}{\sum \frac{\partial \overline{h_1}}{\partial s}\bar{y}_i} \qquad \left(\because \ \frac{d\bar{y}}{dt} = \frac{\partial \bar{y}}{\partial s}\frac{ds}{dt} + \frac{\partial \bar{y}}{\partial t}\frac{dt}{dt} = \frac{\partial \bar{y}}{\partial t}\right) \tag{21}$$

By above differentiation, we can get slope (tangential vector) of surface curve.

tangential vector : $\left(1, \frac{d\bar{z}}{d\bar{y}}\right)$

By rotating tangential vector C.W (Fig.3), we can obtain outward normal vector.

normal vector : $\left(\frac{d\bar{z}}{d\bar{y}}, -1\right)$

Change differential domain Cartesian coordinate to natural coordinate.

$$dS = \sqrt{(d\bar{y})^2 + (d\bar{z})^2} = \sqrt{1 + \left(\frac{d\bar{z}}{d\bar{y}}\right)^2} \ d\bar{y} = \sqrt{1 + \left(\frac{d\bar{z}}{d\bar{y}}\right)^2} \ \frac{d\bar{y}}{ds} \ ds = \sqrt{1 + \left(\frac{\sum \frac{\partial \overline{h_1}}{\partial s}\bar{z}_i}{\sum \frac{\partial \overline{h_1}}{\partial s}\bar{y}_i}\right)^2} \ \left(\sum \frac{\partial \overline{h_1}}{\partial s}\bar{y}_i\right) \ ds \tag{22}$$

③ Outward normal vector & coordinate change at face3 ($\mathrm{at}\ s = 1\ \&\ t = [-1,1]$)

$$\frac{d\bar{y}}{d\bar{z}} = \frac{\partial\bar{y}}{\partial s}\frac{ds}{d\bar{z}} + \frac{\partial\bar{y}}{\partial t}\frac{dt}{d\bar{z}} = \frac{\frac{\partial\bar{y}}{\partial t}}{\frac{\partial\bar{z}}{\partial t}} = \frac{\sum\frac{\partial\overline{h_1}}{\partial t}\overline{y_i}}{\sum\frac{\partial\overline{h_1}}{\partial t}\bar{z}_i} \tag{23}$$

By above differentiation, we can get slope (tangential vector) of surface curve.

tangential vector ： $\left(\frac{d\bar{y}}{d\bar{z}}, 1\right)$

By rotating tangential vector C.W (Fig.3), we can obtain outward normal vector.

normal vector ： $(1, -\frac{d\bar{y}}{d\bar{z}})$

Change differential domain Cartesian coordinate to natural coordinate.

$$dS = \sqrt{(d\bar{y})^2 + (d\bar{z})^2} = \sqrt{\left(\frac{d\bar{y}}{d\bar{z}}\right)^2 + 1}\ \ d\bar{z} = \sqrt{\left(\frac{d\bar{y}}{d\bar{z}}\right)^2 + 1}\ \ \frac{d\bar{z}}{dt}\ \ dt = \sqrt{\left(\frac{\sum\frac{\partial\overline{h_1}}{\partial t}\overline{y_1}}{\sum\frac{\partial\overline{h_1}}{\partial t}\overline{z_1}}\right)^2 + 1}\ \ (\sum\frac{\partial\overline{h_1}}{\partial t}\bar{z}_i\ )\ dt \tag{24}$$

④ Outward normal vector & coordinate change at face4 (at $t = 1$ & $s = [-1,1]$)

$$\frac{d\bar{z}}{d\bar{y}} = \frac{\partial \bar{z}}{\partial s}\frac{ds}{d\bar{y}} + \frac{\partial \bar{z}}{\partial t}\frac{dt}{d\bar{y}} = \frac{\frac{\partial \bar{z}}{\partial s}}{\frac{\partial \bar{y}}{\partial s}} = \frac{\sum \frac{\partial \bar{h}_1}{\partial s}\bar{z}_i}{\sum \frac{\partial \bar{h}_1}{\partial s}\bar{y}_i} \tag{25}$$

By above differentiation, we can get slope (tangential vector) of surface curve.

tangential vector : $\left(1, \frac{d\bar{z}}{d\bar{y}}\right)$

By rotating tangential vector C.C.W (Fig.3), we can obtain outward normal vector.

normal vector : $\left(-\frac{d\bar{z}}{d\bar{y}}, 1\right)$

Change differential domain Cartesian coordinate to natural coordinate.

$$dS = \sqrt{(d\bar{y})^2 + (d\bar{z})^2} = \sqrt{1 + \left(\frac{d\bar{z}}{d\bar{y}}\right)^2}\ d\bar{y} = \sqrt{\left(\frac{d\bar{y}}{d\bar{z}}\right)^2 + 1}\ \frac{d\bar{y}}{ds}\ ds = \sqrt{1 + \left(\frac{\sum \frac{\partial \bar{h}_1}{\partial s}\bar{z}_i}{\sum \frac{\partial \bar{h}_1}{\partial s}\bar{y}_i}\right)^2}\ \left(\sum \frac{\partial \bar{h}_1}{\partial s}\bar{y}_i\right)\ ds \tag{26}$$

By above 4 steps, we can obtain R.H.S of variational formulation (e.q.[14]). Also in multi-element case, inside surface boundary conditions are automatically eliminated each other. Because absolute values are same, and outward normal vectors are opposite each other. (Fig.9)

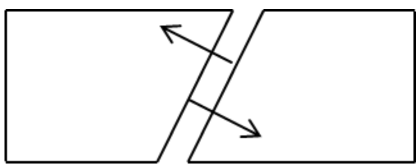

Fig.9. Elimination of inside surface boundary condition

Different coordinate origin gives us different nodal coordinate $\bar{y}_i$, $\bar{z}_i$. By above whole procedure we obtain warping function at origin O Cartesian coordinate (it means rotating center is O). However generally we need warping function at center of twist. Thus, we introduce getting coordinate of twisting center and warping function at twisting center by translating coordinate center.

3.3 Calculation of twisting center with warping function

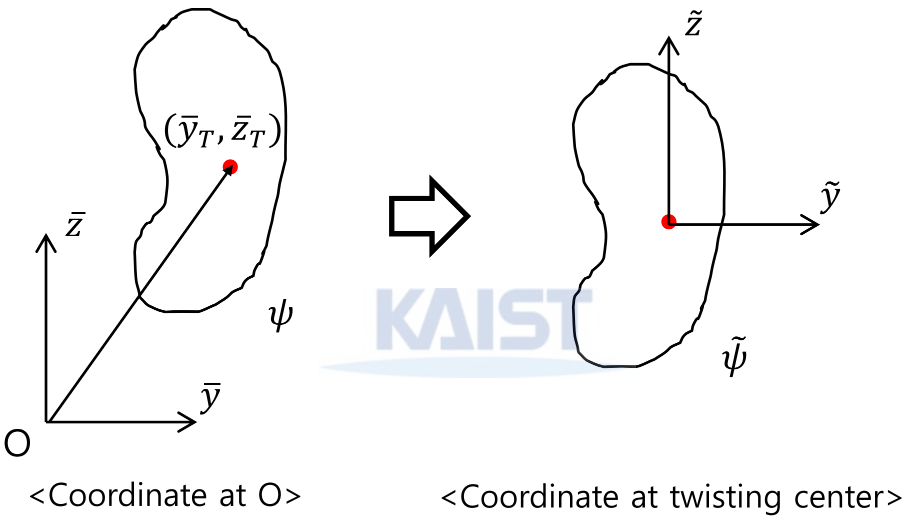

Fig.10. Translation of coordinate center of warping function at twisting center

As previously stated, St.Venant solution has different values according to center of coordinate. However these different values have relation, and are easily changed. Simple translation of coordinate system don`t affect L.H.S of variational formulation (governing equation). Therefore, cause of difference of solution is nodal coordinates $\bar{y}_i$, $\bar{z}_i$ in boundary condition term. For derivation, firstly we define some terms.

ψ : Warping function at O, $\tilde{\psi}$: Warping function at twisting center,

$\bar{y}_T, \bar{z}_T$: coordinates of twisting center

$$\psi_n = \psi - \frac{1}{A}\int \psi dA, \qquad \bar{y}_n = \bar{y} - \frac{1}{A}\int \bar{y} dA, \qquad \bar{z}_n = \bar{z} - \frac{1}{A}\int \bar{z} dA \tag{27}$$

Derivation starts with boundary condition term as following.

$$m\frac{\partial\psi}{\partial\bar{y}} + n\frac{\partial\psi}{\partial\bar{z}} = m\bar{z} - n\bar{y} \tag{28}$$

$$\frac{\partial\psi}{\partial\bar{y}} = \bar{z}, \quad \frac{\partial\psi}{\partial\bar{z}} = -\bar{y} \qquad (\because \text{ m and n are each independent }) \tag{29}$$

State e.q.[29] each center of coordinates at original center O and twisting center.

$$\begin{pmatrix} \frac{\partial\psi}{\partial\bar{y}} = \bar{z}\ , & \frac{\partial\psi}{\partial\bar{z}} = -\bar{y} \\ \frac{\partial\tilde{\psi}}{\partial\bar{y}} = \bar{z} - \bar{z}_T\ , & \frac{\partial\tilde{\psi}}{\partial\bar{z}} = -\bar{y} + \bar{y}_T \end{pmatrix} \qquad (\text{at } \ \partial\Omega\ ) \tag{30}$$

Substitute $\bar{y}$ and $\bar{z}$

$$\frac{\partial\tilde{\psi}}{\partial\bar{y}} = \frac{\partial\psi}{\partial\bar{y}} - \bar{z}_T\ , \quad \frac{\partial\tilde{\psi}}{\partial\bar{z}} = \frac{\partial\psi}{\partial\bar{z}} + \bar{y}_T \tag{31}$$

Integrate above differential equation (e.q.[31])

$$\tilde{\psi} = \psi - \bar{z}_T\bar{y} + C_1(\bar{z}), \qquad \tilde{\psi} = \psi + \bar{y}_T\bar{z} + C_2(\bar{y}) \tag{32}$$

Above two equation give

$$-\bar{z}_T\bar{y} + C_1(\bar{z}) = \bar{y}_T\bar{z} + C_2(\bar{y}) \tag{33}$$

$$\begin{cases} C_1(\bar{z}) = \bar{y}_T\bar{z} + C \\ C_2(\bar{y}) = -\bar{z}_T\bar{y} + C \end{cases} \qquad (\because \text{ identical equation}) \tag{34}$$

Plug in e.q.[32] and e.q.[34].

$$\tilde{\psi} = \psi + \bar{y}_T\bar{z} - \bar{z}_T\bar{y} + C \tag{35}$$

To arrange constant terms with e.q.[27], we obtain e.q.[36].

$$\tilde{\psi} = \psi_n + \bar{y}_T\bar{z}_n - \bar{z}_T\bar{y}_n + C' \tag{36}$$

$$\int \tilde{\psi} dA = \int \psi_n dA = \int \bar{y}_n dA = \int \bar{z}_n dA = 0 \qquad (\because \text{e.q.}[27]) \tag{37}$$

To apply e.q.[37] at e.q.[36], obtain transformation relation.

$$\tilde{\psi} = \psi_n + \bar{y}_T\bar{z}_n - \bar{z}_T\bar{y}_n \tag{38}$$

For getting center of twist, continuously,

$$\begin{aligned} &\int \tilde{\psi}\bar{y}\, dA = \int \tilde{\psi}\bar{y}_n\, dA = \int \psi_n\bar{y}_n + \bar{y}_T\bar{z}_n\bar{y}_n - \bar{z}_T{\bar{y}_n}^2\, dA, \\ &\int \tilde{\psi}\bar{z}\, dA = \int \tilde{\psi}\bar{z}_n\, dA = \int \psi_n\bar{z}_n + \bar{y}_T{\bar{z}_n}^2 - \bar{z}_T\bar{y}_n\bar{z}_n \; dA \end{aligned} \tag{39}$$

Finally, obtain coordinate of twisting center y_D, z_D with define integration product $A_{\psi_n\psi_n} = \int \psi_n^2 dA$.

$$y_D = -\frac{A_{\psi_n\bar{z}_n}A_{\bar{y}_n\bar{y}_n} - A_{\psi_n\bar{y}_n}A_{\bar{y}_n\bar{z}_n}}{A_{\bar{y}_n\bar{y}_n}A_{\bar{z}_n\bar{z}_n} - A_{\bar{y}_n\bar{y}_n}^2}, \quad z_D = \frac{A_{\psi_n\bar{y}_n}A_{\bar{z}_n\bar{z}_n} - A_{\psi_n\bar{z}_n}A_{\bar{y}_n\bar{z}_n}}{A_{\bar{y}_n\bar{y}_n}A_{\bar{z}_n\bar{z}_n} - A_{\bar{y}_n\bar{z}_n}^2} \tag{40}$$

By above derivation, alternative representations with ψ, $\tilde{\psi}$ are possible. We can easily translate rotation center, and get the corresponding warping function.

Chapter 4. Numerical results

We present mathematically indefective formulation by this time. In this section, demonstrate various cases by using Fortran, and optimize sectional finite element model. Through rectangular section case, show improvement of performance and decide optimal sectional model. In open and closed section case, verify results, with analytical solution and MITC4 shell model, for free and restrained warping condition. Also, in distributed torsion problem, verify results likewise. Lastly, eccentric end tip load problem is compared with shell model.

4.1. Rectangular section

We demonstrate rectangular cross section for determining optimized interpolation order and number of elements. accuracy and operating time are in inverse proportion. Accuracy of numerical warping function is determined by sectional interpolation order (number of elemental node), and number of element. Thus we have to optimize these two parameters. Demonstrate condition of beam is as following.

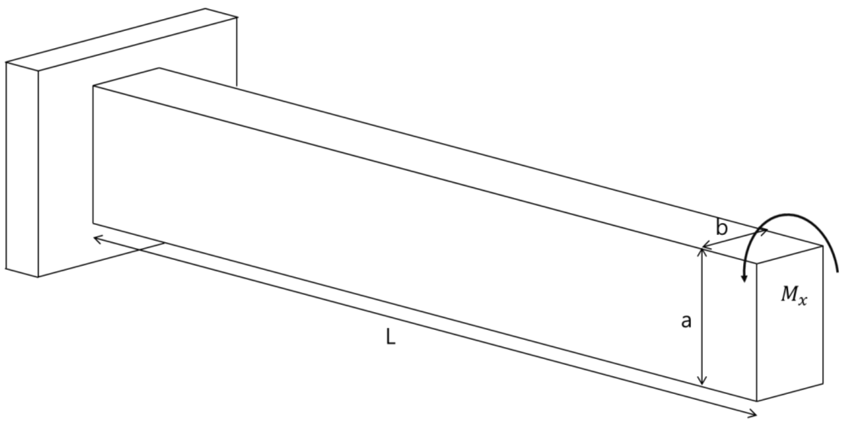

$E = 200 \times 10^9$

$\upsilon = 0.3$

$M_x = 200$

L=20

b=2

Fig.11. Demonstration condition of beam, free warping cantilever with torsion at end tip

4.1.1. Effect of sectional interpolation order

We compare x-directional rotation value, with analytical solution and ADINA, as changing interpolation order and a/b ratio using only one sectional element. (Fig.12) Analytical solutions are obtained by following formulations.

$\theta_x = \frac{M_x L}{GK}$, for square $K = 0.140625a^4$

for rectangle $K = ab^3\left[\frac{16}{3} - 3.36\frac{b}{a}(1 - \frac{b^4}{12a^4})\right]$

for very thin $K = \frac{ab^3}{3}$

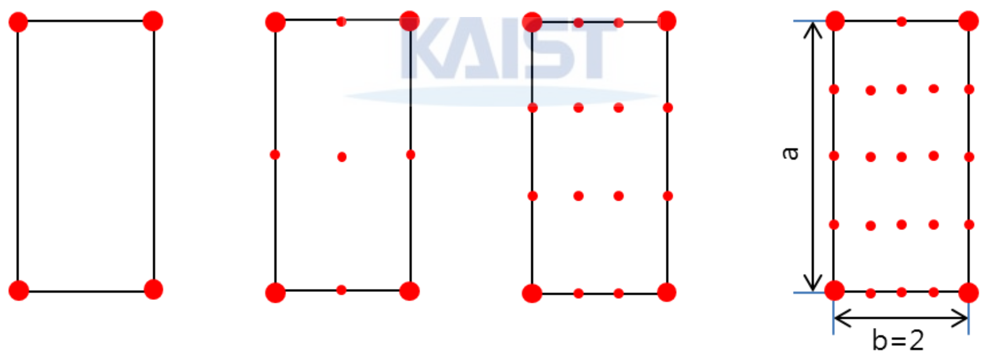

Fig.12. Interpolation condition of rectangular section

Table.1. Result of θ_x as changing slenderness of rectangular section with various interpolation order

(Each cases use only 1 sectional element)

a/b ratio	*Analytical Sol.*	*ADINA*	*1st order Interpol.*	*2nd order Interpol.*	*3rd order Interpol.*	*4th order Interpol.*
1	2.3111E-8	2.309E-8	1.931E-8	1.931E-8	2.309E-8	2.309E-8
2	7.0998E-9	7.047E-9	6.094E-9	6.094E-9	7.080E-9	7.080E-9
4	2.8930E-9	2.816E-9	2.590E-9	2.590E-9	2.846E-9	2.846E-9
10	1.0406E-9	1.006E-9	9.847E-9	9.848E-9	1.011E-9	1.011E-9
100	9.75E-11	9.753E-11	9.751E-11	9.751E-11	9.754E-11	9.754E-11

Through table1 and fig.13, we can know that warping function is reliably spanned by 3rd order polynomial. Also 1st order interpolation can give us accurate solution with slender structure. Thus we select order of interpolation by shape of structure. (Additionally table1 verify us warping function of rectangular section have odd function) And it give us closer value than ADINA`s. Also ADINA use two additional warping degree of freedoms α, β and formulation is as following. (our study is only one additional warping DOF)

$$u_w = yz\alpha + yz(y^2 - z^2)\beta$$

Conclusion is that performance is improved with reduced degree of freedom.

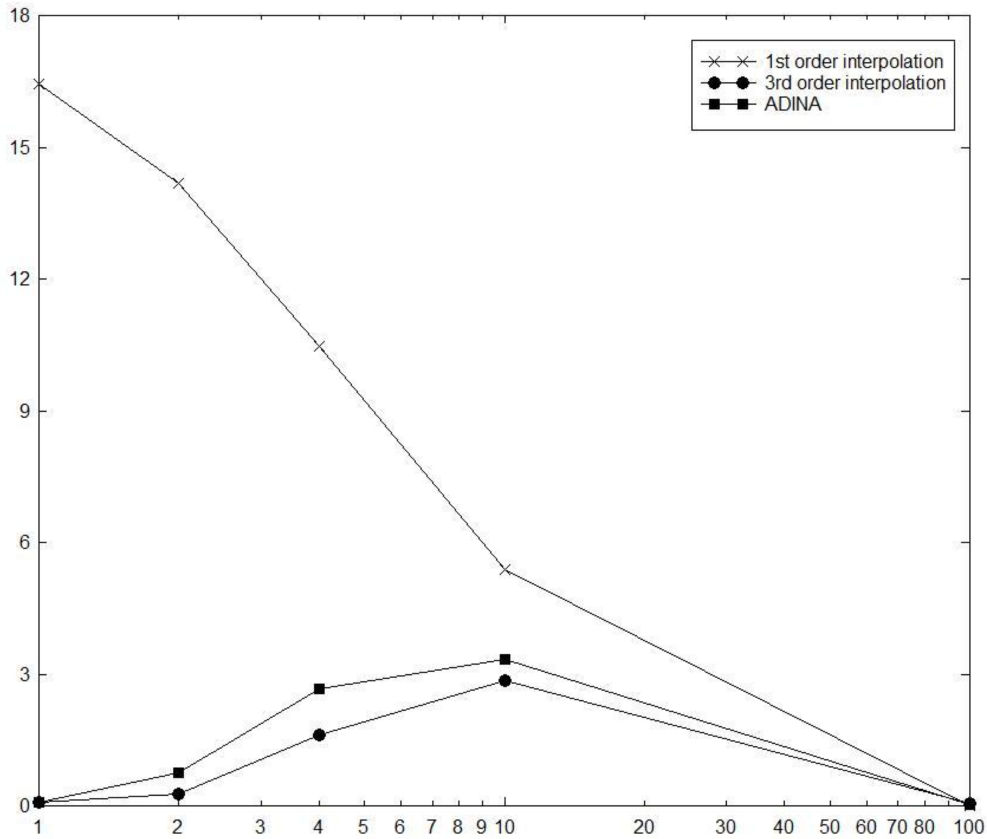

Fig.13. Error curve of rectangular section as changing slenderness ($\mathrm{e} = \left|\frac{(Ref)-\theta_x}{(Ref)}\right|$)

4.1.2. Effect of number of sectional elements

We compare x-directional rotation value as changing number of sectional element. Beam testing condition is same as fig.10 and section condition is as fig.14

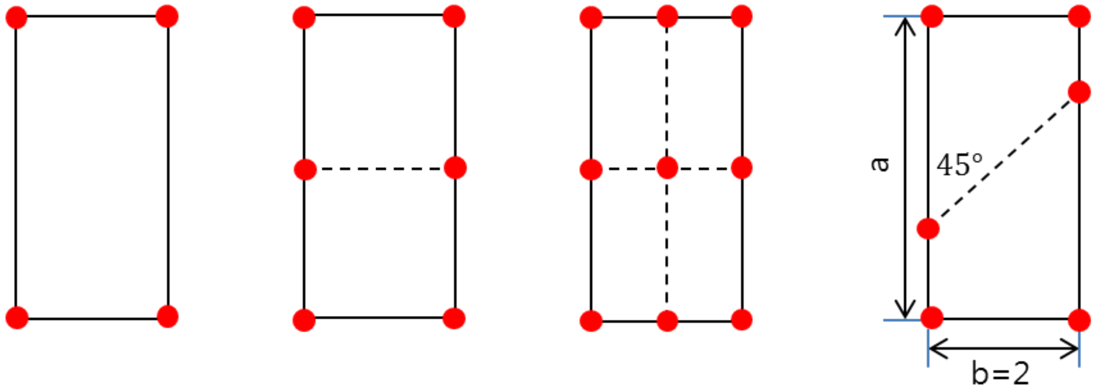

Fig.14. Patched rectangular section condition

Table.2. Result of θ_x as changing number of sectional elements with rectangular section (using 3rd order interpolation)

a/b ratio	*Analytical sol.*	*1 element*	*2 element*	*4element*	*2 element Trapezoid*
1	2.3111E-8	2.3090E-8	2.3102E-8	2.3111E-8	2.3030E-8
2	7.0998E-9	7.0800E-9	7.0970E-9	7.0980E-9	7.0876E-9
4	2.8930E-9	2.8460E-9	2.8760E-9	2.8761E-9	2.8719E-9
10	1.0406E-9	1.0110E-9	1.0218E-9	1.0218E-9	1.0221E-9
100	9.7500E-11	9.7540E-11	9.7558E-11	9.7558E-11	9.7562E-11

By Table.2, finer mesh gives us more accurate result. Thus, with above two results, we can decide that elements number are not important when we use 3rd order interpolation function.

4.2. Free/restrained warping condition for open section (L, I, C)

L, I, and C section beam are abundantly used in engineering structures. And also free/restrained warping analytical solution is well known. Compare x-directional rotation as changing thickness for free warping condition, and as changing number of beam element for restrained warping condition in each 2node and 3node beam element case. In all case, we use 3rd order interpolation.

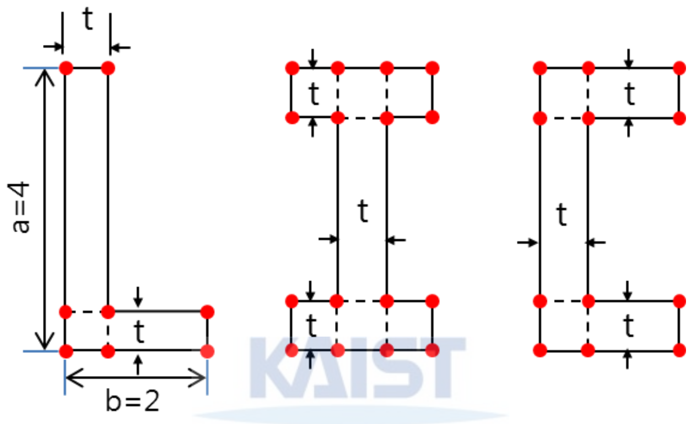

Fig.15. Mesh condition of open section (L, I, C)

4.2.1 Remarks on reference values (shell model and analytical solution)

For verifying performance of present beam elements, we suggest two kind of reference value, analytical solution (Roark`s formulas for stress and strain), and MITC4 shell model. We design shell model which deform most similar behavior to beam elements. We get guarantee of shell model from simple cases, and we use the model as reference value in complex problem that analytical solution is unknown. Method of modeling are as following Fig16, Fig.17.

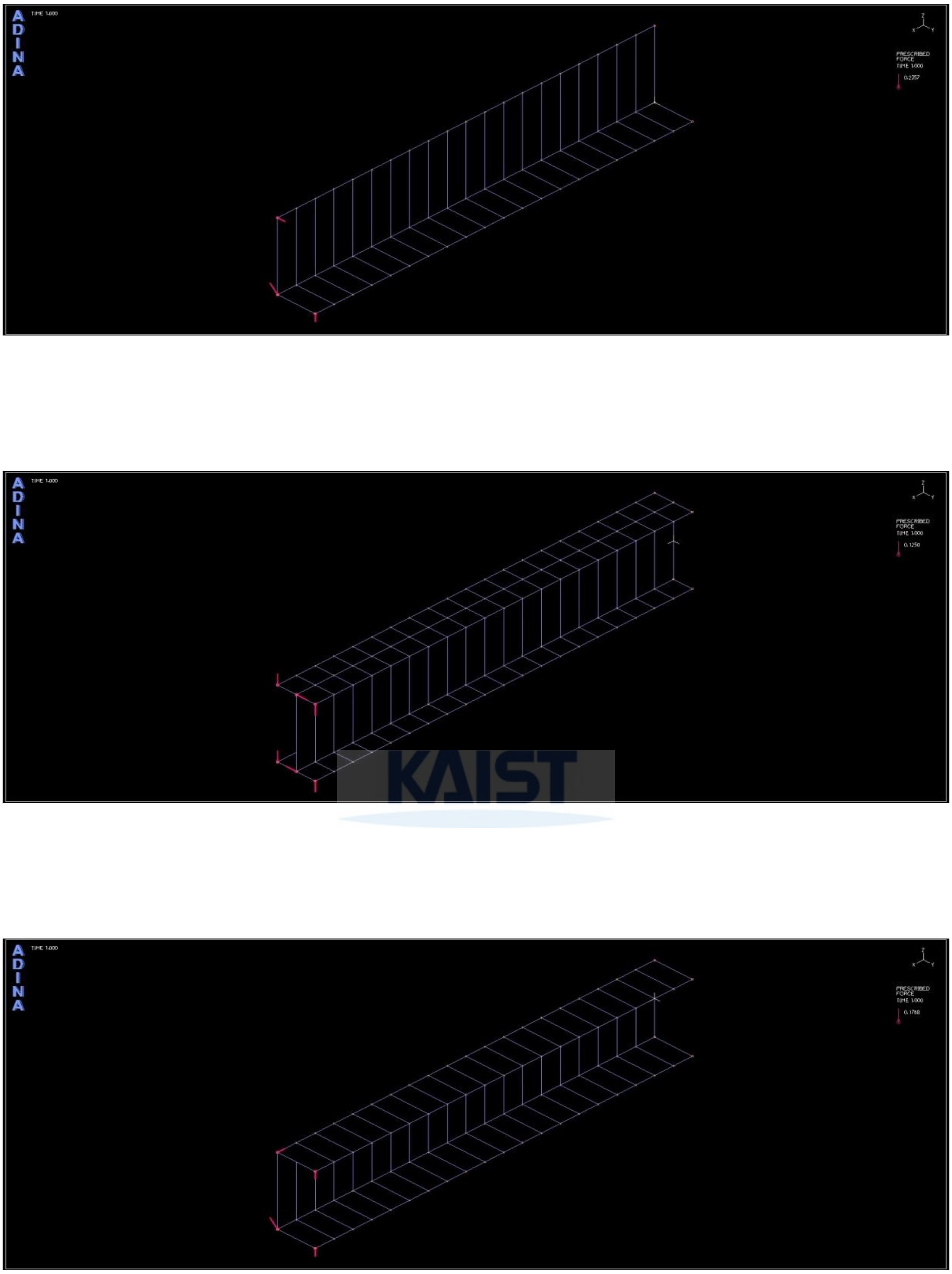

Fig.16. Shell model for L, I, C cross-section

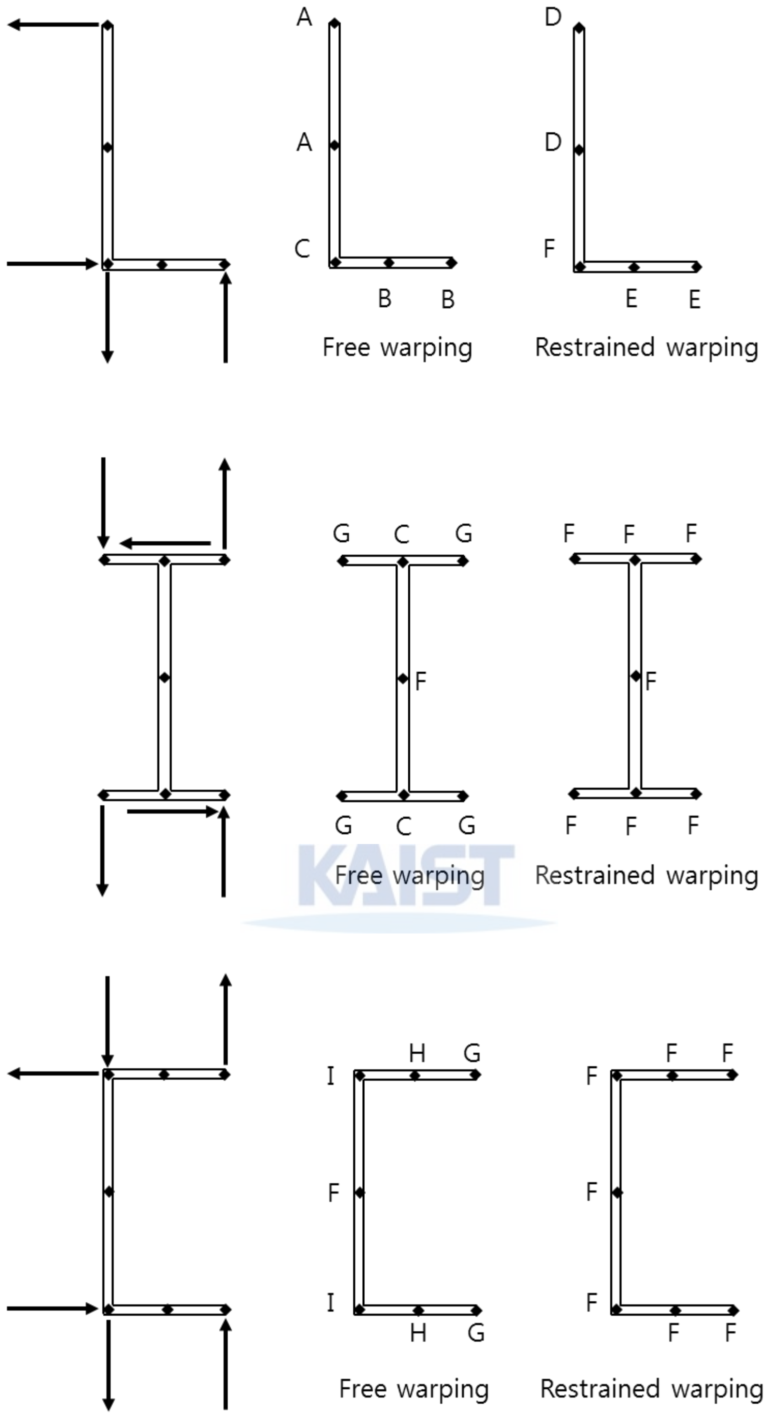

	u	v	w	θ_x	θ_y	θ_z
A	●	●				
B	●		●			
C	●	●	●			
D	●	●			●	●
E	●		●		●	●

	u	v	w	θ_x	θ_y	θ_z
F	●	●	●		●	●
G		●	●			●
H	●	●	●			●
I		●	●			

Fig.17. Boundary condition for L, I, C cross-section

For calculating analytical solution of thin walled beam structures, we use Bredt`s formula in free warping case.

G : shear modulus ,   L : beam length

l_i : *length of leg,* t_i : *thickness of leg*

$$\mathrm{M} = (\frac{G}{L}\sum_{i=1}^{n}\frac{l_i t_i^3}{3}) \cdot \theta$$

In restrained warping, and distributed moment problem, we use ‘Roark`s formulas for stress and strain’.

($\beta = \sqrt{\frac{KG}{C_w E}}$)

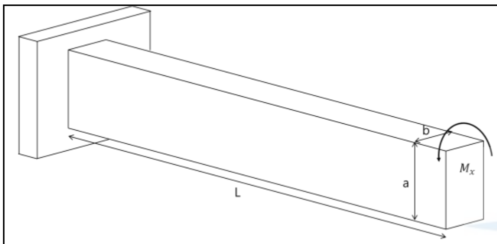 Restrained warping	$\theta_x = \frac{T}{C_w E \beta^3}[\beta(l-x) - tanh\beta l + \frac{sinh\beta x}{cosh\beta l}$
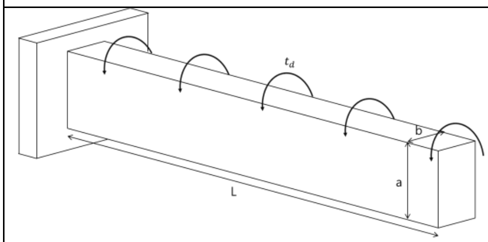 Distributed moment with free warping	$\theta_x = \frac{t}{C_w E \beta^4}[\frac{\beta^2(l^2-x^2)}{2} + \frac{sinh\beta(l-x) + sinh\beta x}{sinh\beta l} - 1]$
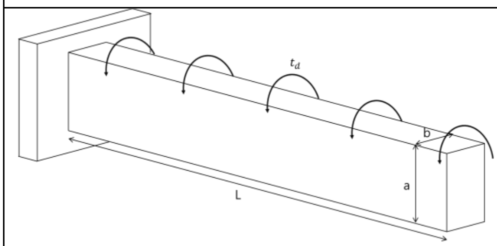 Distributed moment with restrained warping	$\theta_x = \frac{t}{C_w E \beta^4}[\frac{1 - cosh\beta(l-x) + \beta l(sinh\beta l - sinh\beta x)}{cosh\beta l} + \frac{\beta^2(l^2-x^2)}{2}]$

Torsional properties of each section are as following.

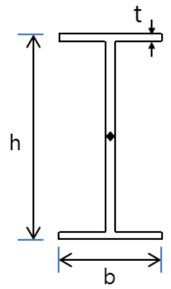	$K = \frac{1}{3}(2t^3 b + t^3 h)$ $C_w = \frac{h^2 t b^3}{24}$
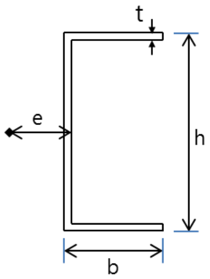	$e = \frac{3b^2}{h + 6b}$ $K = \frac{t^3}{3}(h + 2b)$ $C_w = \frac{h^2 b^3 t}{12} \frac{2h + 3b}{h + 6b}$

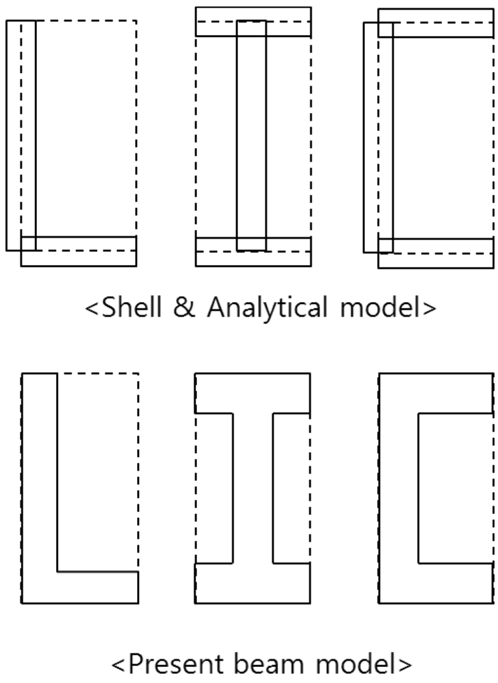

Fig.18 Difference modeling between reference and this study

By difference of modeling (Fig.18), results have to be shown difference. As thickness is increase, result should have more difference. We can see that difference results.

4.2.2. Free warping condition for L, I, C section

Thin walled structure is abundantly used, especially L, I, and C section. We compare results with analytical solutions and MITC4 shell model, as changing thickness of legs. We can generally see that difference of result is larger as increasing thickness (because of difference of model). Demonstrate condition is as following in Fig.19. a, b mean dimension of reference rectangle.

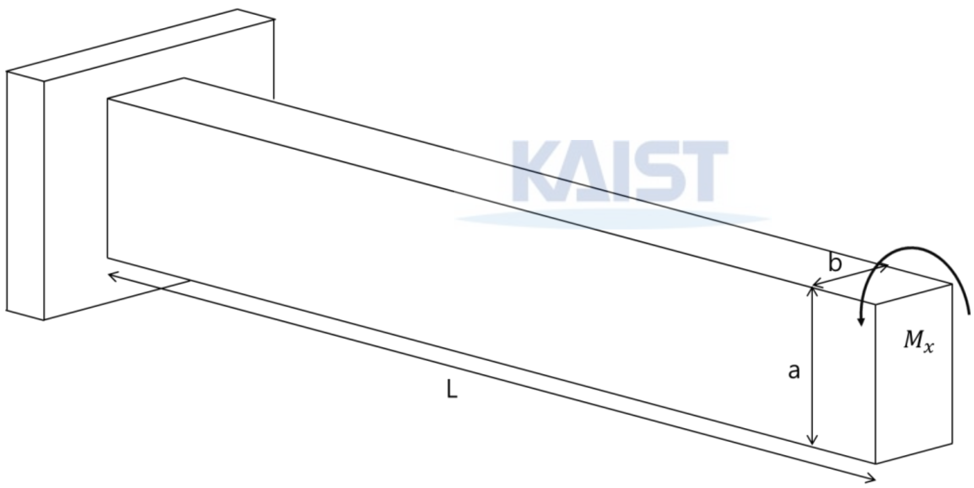

$E = 200 \times 10^9$

$\upsilon = 0$

$M_x = 1$

L=20

b=2

a=4

Fig.19. Demonstration condition of beam, free warping cantilever with torsion at end tip

Each L, I, C sectional demonstration conditions are in Fig.20, Fig.21, Fig.22, and each result are in Table.3, Table4, Table5. We can see C-section occur more difference than I-section. The reason is in Fig.18. C-section has larger area out of reference rectangle.

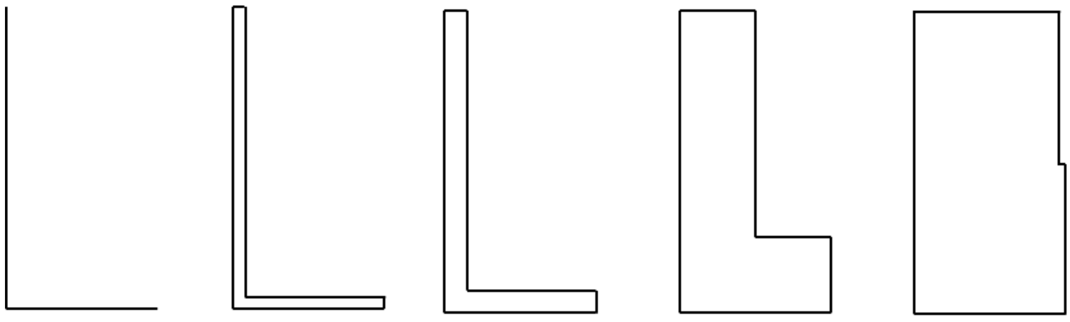

Fig.20. Thickness change of L-section

Table.3. L-section result of θ_x as changing thickness with free warping condition

Thick ness	*Shell solution (only thin case)*	*Analytical solution (only thin case)*	*Present study*	*Difference*
1.99	-	(2.737E-11)	2.7473E-11	-
1	-	-	1.2893E-10	-
0.1	1.0013E-7	1.0000E-7	1.0098E-7	0.980%
0.05	8.0027E-7	8.0000E-7	8.0301E-7	0.376%
0.01	1.0000E-4	1.0000E-4	1.0006E-4	0.06%

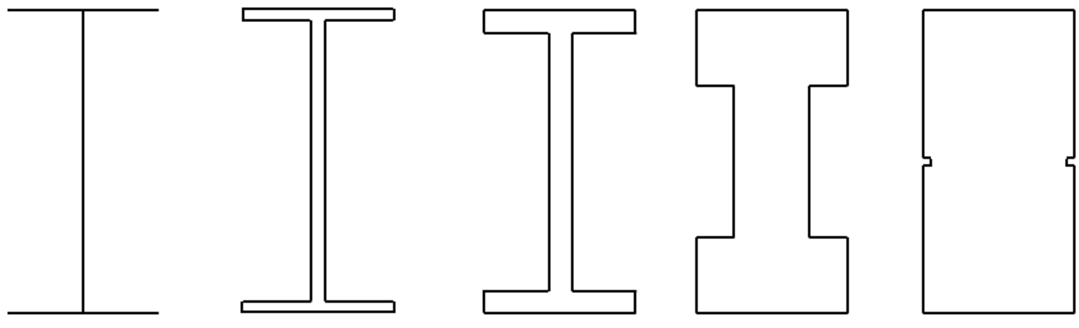

Fig.21. Thickness change of I-section

Table.4. I-section result of θ_x as changing thickness with free warping condition

Thickness	*Shell solution (only thin case)*	*Analytical solution (only thin case)*	*Present study*	*Difference*
1.99	-	(2.737E-11)	2.7300E-11	-
1	-	-	9.5169E-11	-
0.1	7.5159E-8	7.5000E-8	7.4385E-8	0.820%
0.05	6.0035E-7	6.0000E-7	5.9378E-7	1.037%
0.01	7.5002E-5	7.5000E-5	7.4693E-5	0.409%

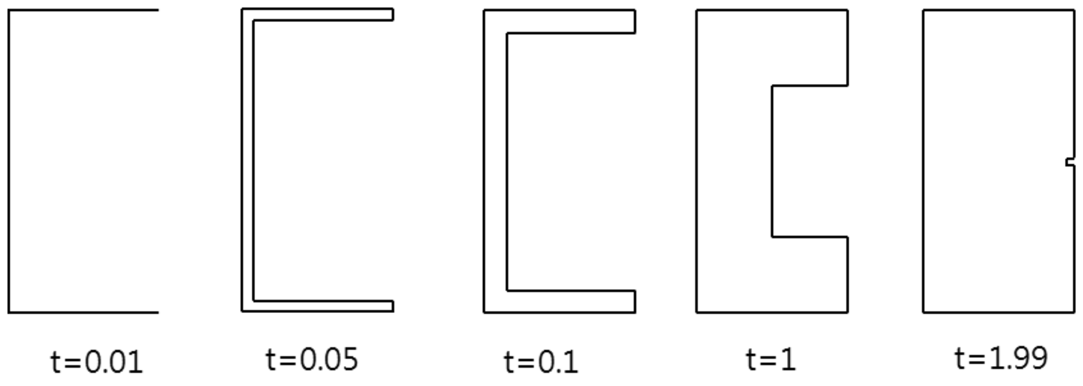

Fig.22. Thickness change of C-section

Table.5. C-section result of θ_x as changing thickness with free warping condition

Thickness	*Shell solution (only thin case)*	*Analytical solution (only thin case)*	*Present study*	*Difference*
1.99	-	(2.737E-11)	2.7300E-11	-
1	-	-	1.0278E-10	-
0.1	7.5116E-8	7.5000E-8	7.6092E-8	1.456%
0.05	6.0023E-7	6.0000E-7	6.0349E-7	0.582%
0.01	7.5001E-5	7.5000E-5	7.5065E-5	0.087%

4.2.3. Restrained warping condition for L, I, C section

We compare results with analytical solutions and MITC4 shell model, likewise above free warping case. Demonstrate condition is as following in Fig.23. In restrained warping condition, that is distinct with free warping condition, warping displacement fields are not constant. It means that x-directional (longitudinal direction) rate of change is occurred. Thus, there are needed some beam elements for convergence of solution. Therefore we demonstrate as changing number of beam elements, and beam interpolation order. 2-node element means 1st order interpolation, and 3-node element means 2nd order interpolation.

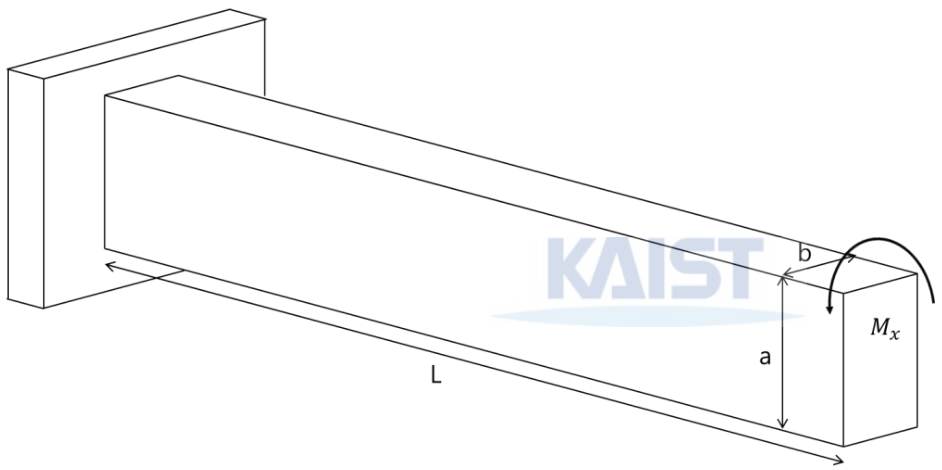

$E = 200 \times 10^9$

$\upsilon = 0$

$M_x = 1$

L=20

b=2

a=4

Fig.23. Demonstration condition of beam, restrained warping cantilever with torsion at end tip

Each L, I, C sectional demonstration conditions are in Fig.20, Fig.21, Fig.22, and each result are in Table.3, Table4, Table5. We can see higher order element gives us quick convergence.

Table.6. L-section result of θ_x as changing thickness with restrained warping condition

(N : the number of elements used)

N \ Thickness	*0.001*		*0.01*		*0.1*	
	2-node	3-node	2-node	3-node	2-node	3-node
1	9.8045E-2	9.5128E-2	9.8103E-5	9.5191E-5	9.9077E-8	9.6207E-8
2	9.4194E-2	9.2953E-2	9.4257E-5	9.3013E-5	9.5276E-8	9.4000E-8
4	9.2936E-2	9.2935E-2	9.2996E-5	9.2996E-5	9.3981E-8	9.3981E-8
8	9.2935E-2	9.2935E-2	9.2996E-5	9.2996E-5	9.3981E-8	9.3981E-8
16	9.2935E-2	9.2935E-2	9.2996E-5	9.2996E-5	9.3981E-8	9.3981E-8
Analytical sol.	-		-		-	
Shell sol.	9.2987E-2		9.2987E-5		9.3111E-8	
Difference	-	-	-	-	-	-

Table.7. I-section result of θ_x as changing thickness with restrained warping condition

(N : the number of elements used)

N \ Thickness	*0.001*		*0.01*		*0.1*	
	2-node	3-node	2-node	3-node	2-node	3-node
1	1.8847E-6	2.5100E-6	1.8886E-7	2.5115E-7	1.5684E-8	1.8633E-8
2	2.3537E-6	2.5100E-6	2.3559E-7	2.5114E-7	1.7909E-8	1.8586E-8
4	2.4709E-6	2.5100E-6	2.4725E-7	2.5114E-7	1.8417E-8	1.8583E-8
8	2.5002E-6	2.5100E-6	2.5017E-7	2.5114E-7	1.8542E-8	1.8583E-8
16	2.5075E-6	2.5100E-6	2.5090E-7	2.5114E-7	1.8573E-8	1.8583E-8
Analytical sol.	2.5000E-6		2.4900E-7		1.7880E-8	
Shell sol.	2.4566E-6		2.4472E-7		1.7692E-8	
Difference	0.304%	0.404%	0.763%	0.859%	3.876%	3.932%

Table.8. C-section result of θ_x as changing thickness with restrained warping condition

(N : the number of elements used)

N \ *Thickness*	*0.001*		*0.01*		*0.1*	
	2-node	3-node	2-node	3-node	2-node	3-node
1	1.0809E-6	1.1112E-6	1.0915E-7	1.1214E-7	1.0528E-8	1.0318E-8
2	1.3490E-6	1.3711E-6	1.3614E-7	1.3834E-7	1.2381E-8	1.2420E-8
4	1.4161E-6	1.4284E-6	1.4289E-7	1.4412E-7	1.2814E-8	1.2876E-8
8	1.4329E-6	1.4375E-6	1.4457E-7	1.4504E-7	1.2921E-8	1.2948E-8
16	1.4370E-6	1.4384E-6	1.4499E-7	1.4513E-7	1.2947E-8	1.2955E-8
Analytical sol.	1.4285E-6		1.4253E-7		1.1634E-8	
Shell sol.	1.3747E-6		1.3718E-7		1.1299E-8	
Difference	0.595%	0.693%	1.697%	1.824%	11.286%	11.355%

4.3. Closed cross-section

Compare x-directional rotation as changing thickness for free warping condition with analytical solution. Introduce how to obtain analytical solution.

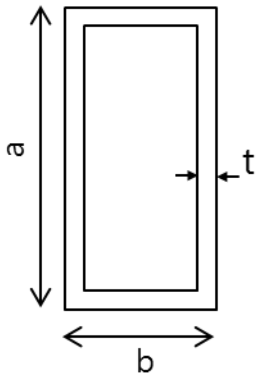

$$K = \frac{2t(a-t)^2(b-t)^2}{at+bt-2t^2}$$

$$\theta_x = \frac{M_x L}{KG}$$

Demonstration beam condition is in Fig.19 same as open section case. Section finite element model and demonstration condition of cross-section is in Fig.24.

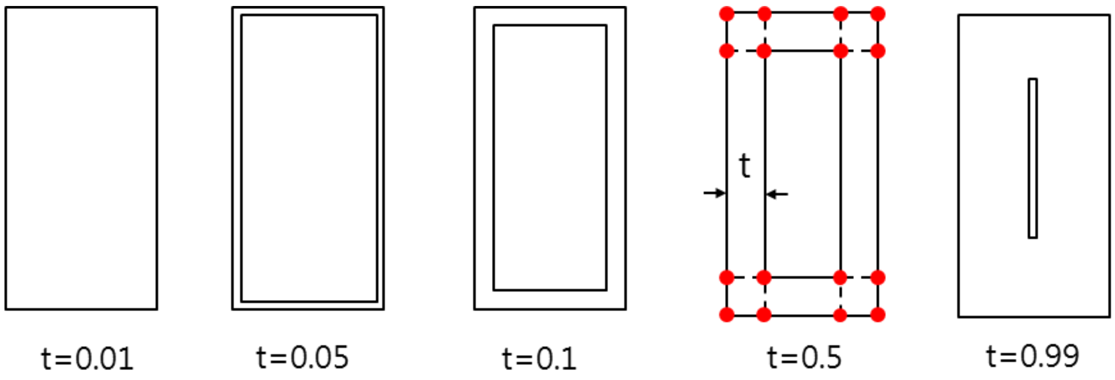

Fig.24 Mesh condition & thickness change of rectangular tube cross-section

Result is in Table.9, and has same tendency with open section cases.

Table.9. Rectangular tube section result of θ_x as changing thickness with free warping condition

Thickness	*Analytical solution (only thin case)*	*Present study*	*Difference*
0.99	(2.737E-11)	2.7426E-11	-
0.5	-	3.1907E-11	-
0.1	1.0563E-10	1.0305E-10	2.443%
0.05	1.9889E-10	1.9616E-10	1.373%
0.01	9.4853E-10	9.4551E-10	0.318%

4.4. Various section

We demonstrate various section, trapezoid, circle, shaft with four splines. Compare x-directional rotation, and testing condition of beam is same as Fig.19. Sectional condition and analytical solutions are in following table.

Section condition	Analytical solution
<Trapezoid> 3rd order 1element 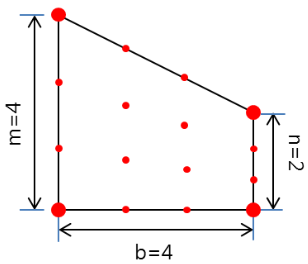 	$K=\frac{1}{12}b(m+n)(m^2+n^2)-V_L m^4-V_s n^4$ $V_L=0.10504-0.1s+0.0848s^2-0.06746s^3+0.0515s^4$ $V_s=0.10504+0.1s+0.0848s^2+0.06746s^3+0.0515s^4$ $s=\frac{m-n}{b}$ $\theta_x=\frac{M_x L}{KG}$
<Circle> 3rd order 1element R=2 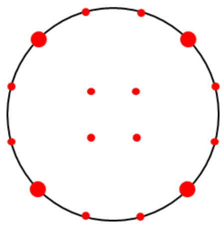	$K=\frac{1}{2}\pi R^4$ $\theta_x=\frac{M_x L}{KG}$
<Shaft with four splines> 3rd order 7element R=2 a=1 b=1 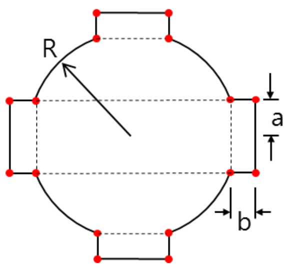 	$K=2CR^4$ $C=K_1+K_2\frac{b}{R}+K_3\left(\frac{b}{R}\right)^2+K_4\left(\frac{b}{R}\right)^3$ $K_1=0.7854$ $K_2=0.0595-0.3397\frac{a}{b}+0.3239\left(\frac{a}{b}\right)^2$ $K_3=-0.6008+3.1396\frac{a}{b}-2.0693\left(\frac{a}{b}\right)^2$ $K_4=1.0869-6.2451\frac{a}{b}+9.4190\left(\frac{a}{b}\right)^2$ $\theta_x=\frac{M_x L}{KG}$

Numerical result is in Table10.

Table.10. Various section result of θ_x free warping condition

	Analytical sol.	*Present study*	*Difference*
Trapezoid	1.0632E-11	1.0845E-11	2.003%
Circle	2.0700E-9	2.0644E-9	0.271%
Shaft with four splines	4.2890E-12	4.6444E-12	8.286%

4.4. Distributed torsion problem

Compare x-directional rotation when uniformly distributed torsional moment is applied. Again, we consider the situations of free and restrained warping condition with L, I, C sections. MITC4 shell models, and analytical solutions are compared with the numerical results. Free/restrained demonstrate conditions of beam are each in Fig25 and Fig.26. Also demonstrate conditions of section are same as section4.2.

4.4.1 Free warping condition for L, I, C section

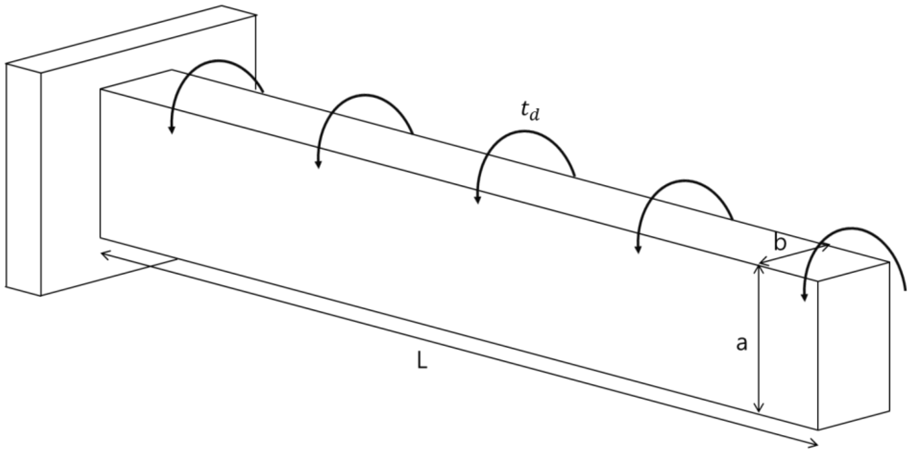

$E = 200 \times 10^9$

$\upsilon = 0$

$t_d = \frac{1}{20}$

L=20

b=2

a=4

Fig.25. Demonstration condition of beam, free warping cantilever with distributed torsion

Table.11. L-section result of θ_x as changing thickness with free warping condition

Thickness	*Shell solution (only thin case)*	*Analytical solution (only thin case)*	*Present study*	*Difference*
1	-	-	6.4466E-11	-
0.1	5.0021E-8	-	5.0495E-8	-
0.05	3.9971E-7	-	4.0156E-7	-
0.01	4.9946E-5	-	5.0029E-5	-

Table.12. I-section result of θ_x as changing thickness with free warping condition

Thickness	*Shell solution (only thin case)*	*Analytical solution (only thin case)*	*Present study*	*Difference*
1	-	-	4.7585E-11	-
0.1	3.6955E-8	3.7500E-8	3.7192E-8	0.821%
0.05	3.0419E-7	3.0000E-7	2.9689E-7	1.037%
0.01	-	3.7500E-5	3.7347E-5	0.408%

Table.13. C-section result of θ_x as changing thickness with free warping condition

Thickness	*Shell solution (only thin case)*	*Analytical solution (only thin case)*	*Present study*	*Difference*
1	-	-	5.1392E-11	-
0.1	3.5713E-8	3.7500E-8	3.8046E-8	1.456%
0.05	2.8539E-7	3.0000E-7	3.0175E-7	0.583%
0.01	3.5661E-5	3.7500E-5	3.7532E-5	0.085%

4.4.2 Restrained warping condition for L, I, C section

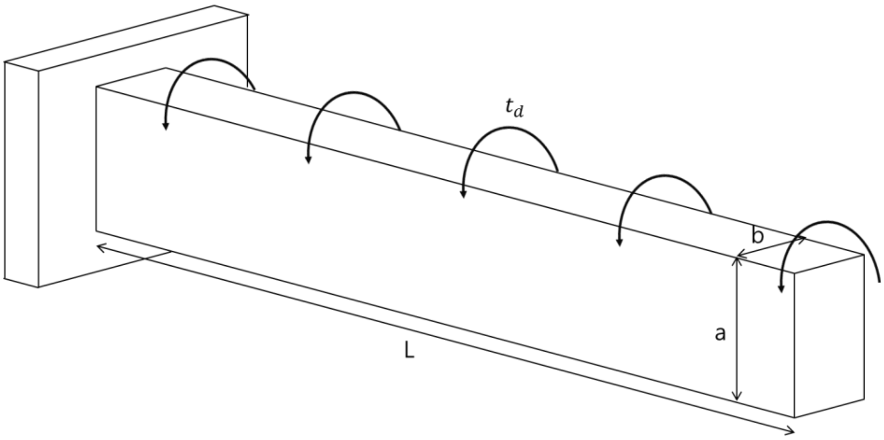

$E = 200 \times 10^9$

$\upsilon = 0$

$t_d = \frac{1}{20}$

L=20

b=2

a=4

Fig.26. Demonstration condition of beam, restrained warping cantilever with distributed torsion

Table.14. L-section result of θ_x as changing thickness with restrained warping condition

(N : the number of elements used)

N \ Thickness	*0.001*		*0.01*		*0.1*	
	2-node	3-node	2-node	3-node	2-node	3-node
1	4.9023E-2	4.5838E-2	4.9051E-5	4.5873E-5	4.9539E-8	4.6408E-8
2	4.4406E-2	4.3899E-2	4.4443E-5	4.3932E-5	4.4987E-8	4.4443E-8
4	4.3427E-2	4.3562E-2	4.3460E-5	4.3595E-5	4.3968E-8	4.4105E-8
8	4.3432E-2	4.3465E-2	4.3465E-5	4.3498E-5	4.3973E-8	4.4006E-8
16	4.3432E-2	4.3440E-2	4.3465E-5	4.3473E-5	4.3973E-8	4.3982E-8
Analytical sol.	-		-		-	
Shell sol.	4.3437E-2		4.3437E-5		4.3509E-8	
Difference	-	-	-	-	-	-

Table.15. I-section result of θ_x as changing thickness with restrained warping condition

(N : the number of elements used)

N \ *Thickness*	*0.001*		*0.01*		*0.1*	
	2-node	3-node	2-node	3-node	2-node	3-node
1	9.4236E-7	1.0205E-6	9.4431E-8	1.0212E-7	7.8422E-9	7.6161E-9
2	9.4235E-7	9.6189E-7	9.4327E-8	9.6254E-8	7.1965E-9	7.1999E-9
4	9.4235E-7	9.4723E-7	9.4306E-8	9.4788E-8	7.0901E-9	7.0940E-9
8	9.4235E-7	9.4357E-7	9.4301E-8	9.4422E-8	7.0662E-9	7.0674E-9
16	9.4235E-7	9.4265E-7	9.4300E-8	9.4330E-8	7.0604E-9	7.0607E-9
Analytical sol.	9.3746E-7		9.3387E-8		6.7764E-9	
Shell sol.	9.4351E-7		9.3997E-8		6.8602E-9	
Error	0.522%	0.554%	0.978%	1.010%	4.191%	4.195%

Table.16. C-section result of θ_x as changing thickness with restrained warping condition

(N : the number of elements used)

N \ *Thickness*	*0.001*		*0.01*		*0.1*	
	2-node	3-node	2-node	3-node	2-node	3-node
1	5.4043E-7	5.8513E-7	5.4574E-8	5.9040E-8	5.2640E-9	5.2975E-9
2	5.4043E-7	5.1793E-7	5.4540E-8	5.2259E-8	4.9708E-9	4.7093E-9
4	5.4043E-7	5.3822E-7	5.4533E-8	5.4307E-8	4.9184E-9	4.8831E-9
8	5.4043E-7	5.4065E-7	5.4531E-8	5.4553E-8	4.9065E-9	4.9045E-9
16	5.4043E-7	5.4057E-7	5.4531E-8	5.4545E-8	4.9035E-9	4.9038E-9
Analytical sol.	5.3570E-7		5.3453E-8		4.3896E-9	
Shell sol.	5.3223E-7		5.3111E-8		4.3955E-9	
Error	0.883%	0.909%	2.017%	2.043%	11.707%	11.714%

4.5. Eccentric load problems

It is hard to encounter pure torsion in practical engineering problem. Equivalent torsion is Usually applied by eccentric load. As increasing number of beam element, we compare v(y-directional displacement), and θ_x(x-directional rotation) with restrained warping cantilever, and end tip eccentric load. (Fig.27) Also compare it along the beam length. (Fig.29, Fig.30) Demonstration condition of section is in Fig.28. With I and C shape section,

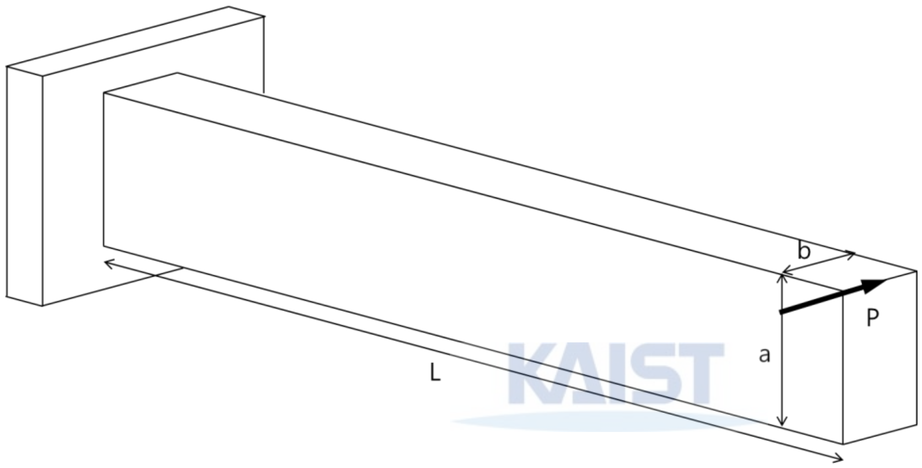

$\mathrm{E} = 200 \times 10^9$

$\upsilon = 0$

$\mathrm{P_y} = 1$

L=20

b=2

a=4

Fig.27. Demonstration condition of beam, restrained warping cantilever with eccentric load at end tip

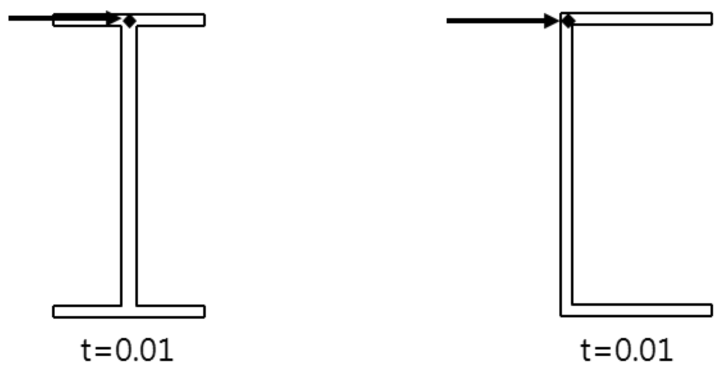

Fig28. Position of eccentric load and thickness in each section

Table.17. Eccentric load for I-section with restrained warping condition

N	*v*		*x-rotation*	
	2-node	3-node	2-node	3-node
1	1.4706E-6	2.0021E-6	-3.6828E-7	-5.0105E-7
2	1.8776E-6	2.0020E-6	-4.7000E-7	-5.0103E-7
4	1.9709E-6	2.0020E-6	-4.9327E-7	-5.0103E-7
8	1.9943E-6	2.0020E-6	-4.9909E-7	-5.0103E-7
16	2.0001E-6	2.0020E-6	-5.0054E-7	-5.0103E-7
Shell sol.	2.0052E-6		-5.0029E-7	

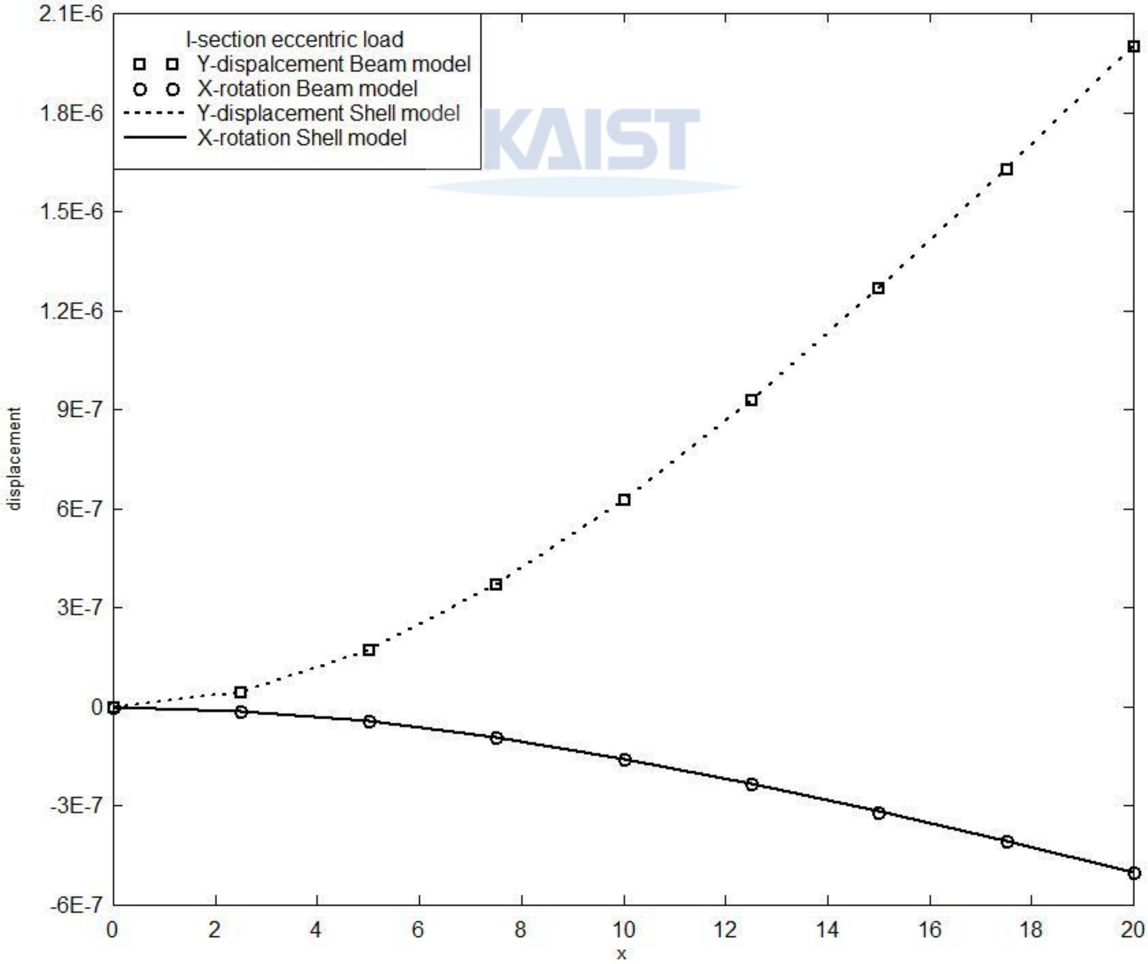

Fig29. Displacements along the beam length with I-section in the eccentric load problem

Table.18. Eccentric load for C-section with restrained warping condition

N	*v*		*x-rotation*	
	2-node	3-node	2-node	3-node
1	7.3917E-7	9.8316E-7	-2.1775E-7	-2.8955E-7
2	9.2218E-7	9.8315E-7	-2.7161E-7	-2.8954E-7
4	9.6791E-7	9.8315E-7	-2.8506E-7	-2.8954E-7
8	9.7934E-7	9.8315E-7	-2.8842E-7	-2.8954E-7
16	9.8220E-7	9.8315E-7	-2.8926E-7	-2.8954E-7
Shell sol.	9.8043E-7		-2.8763E-7	

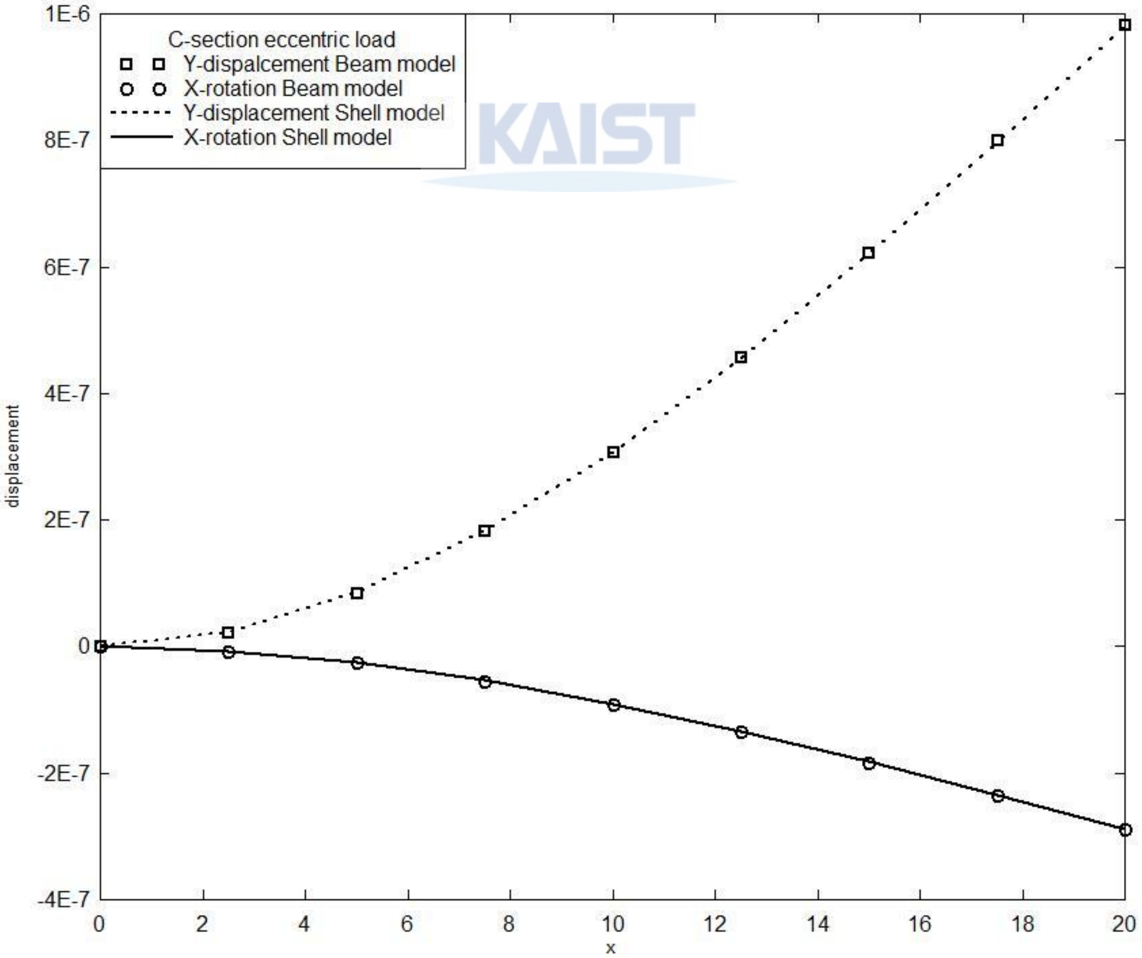

Fig.30. Displacements along the beam length with C-section in the eccentric load problem

Chapter 5. Conclusions

By using numerically obtained warping function, we could improve performance and numerically allow to solve torsional problem for arbitrary section. This paper resolve the problem of beam elements that cross-section have to remain plane (original configuration). But it still has limitation which can describe deformation of cross-section only longitudinal direction. I think it`s possible that solve other directional deformation with certain kinematic formulations.

Suggested method has advantage easy to approach non-linear problems. For considering non-linear behavior, I will study about Wagner effect, and apply our beam elements.

References

[1] Bathe KJ. *Finite element procedure*, New York Prentice Hall; 1996.

[2] Bathe KJ, Chaudhary A. On the displacement formulation of torsion of shafts with rectangular cross-section. *International Journal for Numerical Methods in Engineering*.18,1565-1568, 1982.

[3] Lee PS, McClure G. A general three-dimensional L section beam finite element. *Computer and Structure* 2006;84:215-229.

[4] Vlasov VZ. *Thin-walled elastic beams*, UMI; 1961.

[5] Boresi, Schmidt. *Advanced Mechanics of Materials*, Wiley; 2002.

[6] Gruttmann F. Shwar stresses in prismatic beams with arbitrary cross-section, International journal for numerical methods in engineering, 1999, 45:865-889

[7] Timoshenko S.P. Theory of elasticity, McGraw Hill; 1970

[8] Young WC, Roark`s formulas for stress and strain, McGraw Hill; 1976

Summary

Development of general beam finite elements for arbitrary section with warping displacement

본 논문에서는 유한요소법을 이용하여 임의의 단면을 가지는 빔의 비틀림 문제를 해석할 수 있는 방법론을 제시하였다. 임의의 단면에 대해 고려하기 위해, St.Venant 방정식을 유한요소법을 통해 수치적으로 풀어냈으며, wapring effect 에 의한 연속적인 변위장을 얻기 위해, 각 절점에 warping 자유도를 정의해 앞서 구한 해를 보간 하였다. 이렇게 구해진 변위장을 기존의 3-D 곡률 빔의 변위장에 중첩시켜, 최종적인 변위장을 얻고 이를 통해 복합 변형을 고려 할 수 있는 강성행렬을 구해 낼 수 있다.